

University of Warwick institutional repository: <http://go.warwick.ac.uk/wrap>

This paper is made available online in accordance with publisher policies. Please scroll down to view the document itself. Please refer to the repository record for this item and our policy information available from the repository home page for further information.

To see the final version of this paper please visit the publisher's website. Access to the published version may require a subscription.

Author(s): Jorunn I. B. Bos, Miles R. Armstrong,c,1, Eleanor M. Gilroy,1, Petra C. Boevink,1, Ingo Hein,1, Rosalind M. Taylor, Tian Zhendong,f, Stefan Engelhardt, Ramesh R. Vetukuri, Brian Harrower, Christina Dixelius, Glenn Bryan, Ari Sadanandom, Stephen C. Whisson, Sophien Kamoun,2, and Paul R. J. Birch

Article Title: *Phytophthora infestans* effector AVR3a is essential for virulence and manipulates plant immunity by stabilizing host E3 ligase CMPG1

Year of publication: 2010

Link to published version:

<http://dx.doi.org/10.1073/pnas.0914408107>

Publisher statement: None



Division of Plant Sciences



Professor Paul Birch
Division of Plant Sciences
College of Life Sciences
University of Dundee at SCRI
Invergowrie, Dundee DD2 5DA Scotland
Tel; 01382 562731; Fax: 01382 568578

PNAS MS# 2009-14408

RE: submission of a revised version of our manuscript ('*Phytophthora infestans* effector AVR3a is essential for virulence and manipulates plant immunity by stabilizing host E3 ligase CMPG1', by Bos, Armstrong, Gilroy, Boevink, Hein, Taylor, Tian, Engelhardt, Vetukuri, Harrower, Bryan, Whisson, Sadanandom, Kamoun, Birch)

Dear Editor,

Thank you for the reviewers' comments and the invitation to resubmit a revised version of our manuscript. We were pleased to see that the reviewers recognised the host E3 ligase CMPG1 as an important virulence target of *Phytophthora infestans* and, specifically, of the translocated effector AVR3a. All three referees offered suggestions for additional work to improve the manuscript, which we have tried to meet. A full response to the referees' comments is attached and we feel that additional work we have undertaken has shed further light on the interaction between effector and target.

The issue that you raised in response to the referees' comments concerned whether our findings provide sufficient novelty to warrant publication in *PNAS*. We are aware that bacteria and viruses have been shown to manipulate the UPS in both animal and plant hosts, and were not claiming primacy in this regard. Indeed, we cited reviews on this subject, and have included additional citations specific to the bacterial type III effector AvrPtoB, which has been shown, via a series of papers, to act as an E3 ligase in plant hosts. However, we maintain that an equivalent understanding of the targets of effectors from eukaryotic plant pathogens, such as fungi and oomycetes, is not evident from the literature. This is despite their overwhelming importance as the major causes of plant disease, and despite the large size of the corresponding research community. Recently, it has become evident that fungi and oomycetes potentially deploy hundreds of effectors which can enter the host cell, and yet we do not yet know what they do. Determining how these organisms cause diseases is critical to finding ways to combat them, and essential to a fundamental understanding of whether they indeed need to manipulate the same targets and processes in plant hosts as the prokaryotes do. It is extremely important, and we believe of general interest, to show that there may be parallels between the virulence mechanisms of eukaryotic and prokaryotic plant pathogens, despite the obvious differences in their life styles and the evolutionary distance between them.


The main points of novelty in our findings are: 1) the interaction with and stabilization of a plant host E3 ligase by a eukaryotic plant pathogen effector to promote virulence is a novel activity. Indeed, as pointed out by reviewer 2, to date no effector protein has been described to interact with and stabilize a plant E3 ligase to promote virulence. 2) AVR3a is critical to *P. infestans* pathogenicity, as evidenced by the significantly reduced virulence phenotype of the knock-down transformant. 3) AVR3a is the first translocated effector of a filamentous plant pathogen for which a virulence target is described. We believe this is important, and of general interest, for the reasons stated above.

We look forward to your response.

Yours sincerely,

A handwritten signature in blue ink that reads "Paul Birch". The signature is written in a cursive style with a large initial 'P'.

Paul Birch
University of Dundee

A handwritten signature in blue ink that reads "Sophien Kamoun". The signature is written in a cursive style with a large initial 'S'.

Sophien Kamoun
The Sainsbury Laboratory, Norwich

***Phytophthora infestans* effector AVR3a is essential for virulence and manipulates plant immunity by stabilizing host E3 ligase CMPG1**

Jorunn IB Bos¹, Miles R Armstrong^{2,5,8}, Eleanor M Gilroy^{2,8}, Petra C Boevink^{2,8}, Ingo Hein^{3,8}, Rosalind M Taylor^{2,4}, Tian Zhendong^{2,6}, Stefan Engelhardt^{2,5}, Ramesh R Vetukuri^{2,7}, Brian Harrower³, Christina Dixelius⁷, Glenn Bryan³, Ari Sadanandom⁴, Stephen C Whisson², Sophien Kamoun^{1*}, Paul R J Birch^{2,5*}

¹The Sainsbury Laboratory, John Innes Centre, Colney, Norwich, NR4 7UH, UK

²Plant Pathology, and ³Genetics Programmes, Scottish Crop Research Institute, Invergowrie, Dundee DD2 5DA, UK.

⁴Institute of Biomedical and Life Sciences, Bower Building, University of Glasgow, G12 8QQ, UK.

⁵Division of Plant Sciences, College of Life Sciences, University of Dundee at SCRI, Invergowrie, Dundee DD2 5DA, UK

⁶Huazhong Agricultural University, Wuhan, 430070, China

⁷Uppsala BioCenter, Department of Plant Biology and Forest Genetics, University of Agricultural Sciences, Box 7080, 750 07 Uppsala, Sweden

⁸These authors contributed equally to this work

*Authors for correspondence, email: pbirch@scri.ac.uk; sophien.kamoun@sainsbury-laboratory.ac.uk

Running title: AVR3a targets the host ubiquitin proteasome system

Fungal and oomycete plant pathogens translocate effector proteins into host cells to establish infection. However, virulence targets and modes-of-action of their effectors are unknown. Effector AVR3a from potato blight pathogen *Phytophthora infestans* is translocated into host cells and occurs in two forms: AVR3a^{KI}, which is detected by potato resistance protein R3a, strongly suppresses INF1-triggered cell death (ICD), whereas AVR3a^{EM}, which evades recognition by R3a, weakly suppresses host ICD. Here we show that AVR3a interacts with and stabilizes host U-box E3 ligase CMPG1, which is required for ICD. In contrast, AVR3a^{KI/Y147del}, a mutant with a deleted C-terminal tyrosine residue that fails to suppress ICD, cannot interact with or stabilize CMPG1. CMPG1 is stabilized by the inhibitors MG132 and epoxomicin, indicating that it is degraded by the 26S proteasome. CMPG1 is degraded during ICD. However, it is stabilized by mutations in the U-box that prevent its E3 ligase activity. In stabilizing CMPG1, AVR3a thus modifies its normal activity. Remarkably, given the potential for hundreds of effector genes in the *P. infestans* genome, silencing *Avr3a* compromises *P. infestans* pathogenicity, implying that AVR3a is essential for virulence. Interestingly, *Avr3a* silencing can be complemented by *in planta* expression of *Avr3a*^{KI} or *Avr3a*^{EM}, but not the *Avr3a*^{KI/Y147del} mutant. Our data provide genetic evidence that AVR3a is an essential virulence factor that targets and stabilizes the plant E3 ligase CMPG1, potentially to prevent host cell death during the biotrophic phase of infection.

'\body'

Introduction

Two layers of inducible plant defense provide obstacles to infection. Pathogen-associated molecular pattern (PAMP)-triggered immunity (PTI) follows the perception of conserved microbial molecules at the surface of plant cells (1,2). Plant pathogens secrete effector proteins that suppress PTI. Bacteria use a type III secretion system (T3SS) to 'inject' effectors inside host cells. Characterization of the targets of bacterial T3SS effectors has revealed several biochemical mechanisms for host target modification, including manipulation of the ubiquitin proteasome system (UPS) (1-4).

Effectors may be recognized by plant disease resistance (R) proteins, resulting in effector triggered immunity (ETI) that often involves the hypersensitive response (HR), a form of programmed cell death (PCD), coinciding with restriction of the invading pathogen (1). Consequently, many pathogen effectors have evolved to suppress PCD as a component of either PTI or ETI. (1,2).

Oomycetes are eukaryotic microbes that include many devastating plant pathogens. They secrete RXLR effectors that are translocated inside host cells (5-11). The conserved motif RXLR (where R is arginine, X is any amino acid, and L is leucine) in these effectors is required for their translocation (7). RXLR effector AVR3a from *Phytophthora infestans* is represented by two alleles encoding secreted proteins that differ by only two amino acids. AVR3a^{K801I03} (AVR3a^{KI}), but not AVR3a^{E80M103} (AVR3a^{EM}) activates potato resistance protein R3a to trigger ETI (12). In addition, both forms suppress PCD induced by the *P. infestans* elicitor, infestin 1 (INF1); AVR3a^{KI} does so strongly, whereas suppression by AVR3a^{EM} is weak (13,14). INF1 triggers a range of defence responses, including PCD in diverse plant species (15), and shares many features with PAMPs (16-18).

Recently, we have shown that deletion of the C-terminal tyrosine (Y) at position 147 of AVR3a^{KI}, or its replacement by the non-conservative amino acid serine (Y147S), whilst not affecting recognition by R3a, abolishes AVR3a^{KI} ability to suppress INF1-triggered cell death (ICD), allowing these two effector properties to be distinguished. In contrast, conservative replacement of Y147 by phenylalanine (Y147F) does not impact on ICD suppression (14).

The aim of this research was to investigate the molecular process underlying ICD suppression by AVR3a. We show that AVR3a^{KI} strongly interacts with and stabilizes, *in planta*, the host ubiquitin E3-ligase CMPG1. CMPG1 is required for cell death mediated by INF1 (19). Stabilization and interaction are weak with AVR3a^{EM}, and are lost with the AVR3a^{KI/Y147del} mutant, strongly linking suppression of ICD by AVR3a with CMPG1 interaction and stabilization. Stable silencing of *Avr3a* compromises pathogenicity. This loss of virulence is readily complemented by transient expression in host cells of either *Avr3a*^{KI} or *Avr3a*^{EM}, but not the *Avr3a*^{KI/Y147del} mutant, indicating that *Avr3a* is essential for pathogenicity, and providing genetic evidence that CMPG1 is a key virulence target of *P. infestans*.

Results and Discussion

AVR3a interacts with and stabilizes potato E3 ubiquitin ligase CMPG1

To investigate the molecular mechanisms underlying AVR3a-mediated cell death suppression, we identified potential host protein targets using yeast-two-hybrid assays. We independently screened the AVR3a^{KI} and AVR3a^{EM} forms as baits against a prey library from a combination of RNA prepared at 15 hours post-inoculation (hpi) (early biotrophic phase), and at 72 hpi (necrotrophic phase) of a compatible (susceptible) potato interaction. Several distinct candidate AVR3a-interacting host proteins were identified (Table S1). A number of prey clones encoded a potato homologue of CMPG1 that is missing the N-terminal 29 amino acids (Δ N-StCMPG1a; Fig. S1). CMPG1 is an ubiquitin E3-ligase which is required for cell death triggered by a range of pathogen elicitors, including INF1 [19], and is thus a potential target to explain suppression of ICD by AVR3a^{KI} [13]. Consistent with AVR3a^{KI} suppressing such cell death through interaction with CMPG1, the C-terminal portion of AVR3a^{KI}, with or without RXLR-EER sequences, the AVR3a^{KI/Y147F} substitution and AVR3a^{EM}, interacted with CMPG1 using Y2H, whereas no such interaction was observed with either AVR3a^{KI/Y147S} or AVR3a^{KI/Y147del} forms (Fig. 1A).

Attempts to observe *in planta* protein expression of epitope-tagged CMPG1 revealed that it was not, or was only weakly, detected using western blot analyses and thus has low steady state levels under the experimental conditions used. In contrast, CMPG1 was stable in yeast in the absence of AVR3a^{KI} (Fig 1B). To test whether AVR3a alters the steady state levels of CMPG1 *in*

planta, *Agrobacterium tumefaciens* strains expressing 4x-myc-tagged CMPG1 from *Solanum tuberosum* (StCMPG1) were co-infiltrated with strains delivering constructs expressing FLAG-tagged AVR3a^{KI}, AVR3a^{EM}, AVR3a^{KI/Y147del} or a vector control in *Nicotiana benthamiana*. Western blot analysis of leaf tissues harvested at 2, 3 and 5 days post-infiltration (dpi) showed that the ΔN-StCMPG1a protein was stabilized in the presence of AVR3a^{KI} at 3 dpi (Fig. 1C). By 5 dpi, both AVR3a^{KI} and AVR3a^{EM}, but not AVR3a^{KI/Y147del}, stabilized CMPG1 equally well compared to the vector control (Fig. 1D). This suggests that AVR3a^{KI} has stronger CMPG1 stabilization activity than AVR3a^{EM}, consistent with its stronger ICD suppression activity. The failure of AVR3a^{KI/Y147del} to stabilize CMPG1 is consistent with its loss of ICD suppression. Interestingly, AVR3a-stabilized CMPG1 was detected as a double band by western analyses, suggesting that CMPG1 may be modified.

AVR3a^{KI} and AVR3a^{EM}, but not the AVR3a^{KI/Y147del} mutant, also stabilized, at 5 dpi, StCMPG1b (Fig. 1E), a full length CMPG1 protein from *S. tuberosum* that differs by 11 amino acids from StCMPG1a (Fig. S1). However, stabilization of full length StCMPG1b was reduced compared to a truncated version, ΔN-StCMPG1b, which is missing the 29 N-terminal amino acids (Fig. 1E). In addition, full length proteins encoded by two different *CMPG1* genes from *N. benthamiana* (Nb) and one from *S. lycopersicum* (Sl) (Fig. S1), two plants that are hosts for *P. infestans*, were also stabilized at 5 dpi by AVR3a^{KI} and AVR3a^{EM}, but not by AVR3a^{KI/Y147del} upon co-expression in *N. benthamiana* (Fig. S2A).

To independently verify that AVR3a^{KI} more strongly stabilizes CMPG1, *CFP-Avr3a^{KI}*, *CFP-Avr3a^{EM}* and *CFP-Avr3a^{KI/Y147del}* constructs (generating N-terminal fusions to cyan fluorescent protein [CFP]) were each co-expressed with *StCMPG1b-YFP* (expressing full-length StCMPG1b fused to YFP) and visualized at 2 and 3 dpi using confocal microscopy. Whereas CFP fluorescence was similar in each experiment, indicating similar levels of CFP-AVR3a^{KI}, CFP-AVR3a^{EM} and CFP-AVR3a^{KI/Y147del} proteins, CMPG1-YFP fluorescence was significantly stronger following co-expression with CFP-AVR3a^{KI} than with CFP::AVR3a^{EM}, and barely detectable with CFP-AVR3a^{KI/Y147del}, again indicating that AVR3a^{KI} more strongly stabilizes CMPG1 (Fig. S2B-D).

Further analysis *in planta* of the interaction was performed with bimolecular fluorescence complementation (BiFC). N- or C-terminus-encoding portions of *YFP* were fused to *Avr3a^{KI}*, *Avr3a^{EM}*, *Avr3a^{KI/Y147del}*, or full length *StCMPG1b*, and constructs containing complementary

halves of YFP were co-expressed in *N. benthamiana*. Whereas combinations of *StCMPG1-N/C-YFP* with corresponding *N/C-YFP-Avr3a^{KI}* fusions yielded strong fluorescence, measured using a fluorimeter (Fig. 1F), and assessed using confocal microscopy (Fig. 1G), fluorescence was weak following co-expression of *StCMPG1-N/C-YFP* fusions with *N/C-YFP-Avr3a^{EM}* fusions, and barely detectable with *N/C-YFP-Avr3a^{KI/Y147del}* fusions (Fig. 1F; 1G). To investigate whether these differences were due to stabilisation of CMPG1 by the non-mutant forms of AVR3a, *StCMPG1-N/C-YFP* fusions were also co-expressed with either *N/C-YFP-Avr3a^{KI}* or *N/C-YFP-Avr3a^{KI/Y147del}* fusions in the presence of untagged *AVR3a^{KI}* (to stabilize CMPG1), and again showed strong fluorescence only with co-expression of *StCMPG1-N/C-YFP* and *N/C-YFP-Avr3a^{KI}* fusions (Fig. S2E). These results support the lack of interaction between *AVR3a^{KI/Y147del}* and CMPG1 seen in Y2H, and suggest that interaction *in planta* between *AVR3a^{KI}* and CMPG1 is stronger than that observed between *AVR3a^{EM}* and CMPG1.

The inability of the *AVR3a^{KI/Y147del}* mutant to interact with and stabilize CMPG1 is consistent with previous observations that this mutant is unable to suppress ICD [14]. Moreover, the weak stabilization of CMPG1 by *AVR3a^{EM}* corresponds to weak inhibition of INF1-triggered PCD, further supporting the deduction that AVR3a suppresses ICD through its action on CMPG1. Although the *AVR3a^{KI/Y147del}* mutant fails to interact with or stabilize CMPG1, it nevertheless triggers R3a-mediated HR [14; Fig. S2; S3], indicating that CMPG1 is not involved in this defense response. Indeed, silencing of *NtCMPG1* by RNAi did not compromise R3a-triggered HR (Fig. S3), demonstrating that CMPG1 is not a ‘guardee’ mediating recognition of *AVR3a^{KI}* by R3a [20]. Taken together, our data indicate that CMPG1 is a host target of AVR3a and is stabilized by it *in planta*.

Stabilization of CMPG1 also occurs following its inactivation

If suppression of ICD by AVR3a is due to stabilization of CMPG1, we hypothesized that, during ICD, CMPG1 steady state levels should not increase in the absence of AVR3a. As expected, co-expression of 4xmyc-ΔN-*StCMPG1a* with INF1 did not stabilize CMPG1 compared with the vector control at the onset of cell death symptoms (3dpi), while *AVR3a^{KI}* did (Fig. 2A). This was confirmed by co-expression of *INF1* with *StCMPG1b-YFP*, in which no YFP fluorescence was detected throughout a time-course of 1 to 3 dpi, prior to INF1-triggered cell death. Thus, CMPG1-mediated cell death does not require CMPG1 stabilization.

An explanation for the low abundance of CMPG1 in the absence of AVR3a is that it is degraded by the 26S proteasome. We therefore tested whether the 26S proteasome inhibitors MG132 and epoxomicin could stabilize CMPG1. We expressed 4xmyc- Δ N-StCMPG1a in the presence of MG132, epoxomicin, or buffer control. In the absence of AVR3a^{KI}, we observed an increase in CMPG1 protein levels after MG132 (Fig. 2B) and epoxomicin (Figure 2C-E) treatments, indicating that degradation of CMPG1 is dependent on the 26S proteasome. The epoxomicin treatment resulted in stronger stabilization of CMPG1, and a double band reminiscent of stabilization in the presence of AVR3a^{KI} (Fig. 2C).

Since CMPG1 is constantly degraded by the 26S proteasome, we tested whether mutations C37A and W64A in full length NbCMPG1a, previously shown to abolish E3 ligase activity *in vitro* and to act as ‘dominant negatives’ to prevent ICD [19], affected CMPG1 stability. As expected, co-expression of NbCMPG1a (Fig. S1) with AVR3a^{KI} in *N. benthamiana* resulted in stabilization compared to the vector control (Fig. 2F). In the absence of AVR3a, NbCMPG1aC37A and NbCMPG1aW64A proteins were detectable at higher levels than the wild-type protein, suggesting that the mutations in the U-box domain stabilized CMPG1. However, in the presence of AVR3a these inactive forms of CMPG1 were more strongly stabilized and modified, as indicated by the upper band in westerns (Fig 2F). Stabilization of CMPG1 following inactivation of the U-box implies that its E3 ligase activity contributes to its instability, possibly through self-ubiquitination and degradation. The further stabilization and modification by AVR3a may be explained by its action on endogenous, wild-type CMPG1 in this transient expression assay.

With AVR3a, like with epoxomicin, we see accumulation of a modified form of CMPG1. Critically, in order to prevent ICD, these experiments indicate that stabilization of CMPG1 by AVR3a is consistent with modification of its activity to prevent the normal degradation of itself, and thus, potentially, its substrates in the host cell.

CMPG1 activity is important for *P. infestans* pathogenicity

To determine the role of CMPG1 during *P. infestans* infection, we first confirmed the biological significance of CMPG1 stabilization by AVR3a. We detected CMPG1 stabilization in *P. infestans*-infected *N. benthamiana* leaves that were transiently expressing 4xmyc- Δ N-StCMPG1a (Fig. 3A, 3B). Stabilization was detected with isolate 88069 (AVR3a^{EM} homozygote) and isolate

CA65 (*AVR3a^{KI}* homozygote). Although *AVR3a^{EM}* exhibits weaker ICD suppression activity compared to *AVR3a^{KI}* in transient over-expression assays, it is possible that in a natural infection this activity is sufficient for *AVR3a* virulence function.

At the onset of infection we observed that *NbCMPG1* transcripts accumulated rapidly following inoculation of *P. infestans* onto leaves (Fig. S4). This is consistent with previous reports of rapid *CMPG1* up-regulation [19, 21] and suggests that *CMPG1* may contribute to PTI. *Avr3a* is transcriptionally up-regulated in germinating cysts, and during the first 1-3 dpi ([12]; Fig. S4), indicating that its synthesis coincides with early up-regulation of *CMPG1*. As observed previously [23], *INF1* transcript decreased during the biotrophic phase (Fig. S4). This indicates that, in addition to early targeting of *CMPG1* by *AVR3a*, *P. infestans* subsequently reduces its potential to elicit *CMPG1*-mediated PCD during biotrophy, which is consistent with evasion of PTI. In support of this, it has been shown previously that an isolate of *P. infestans* that is silenced for *INF1* expression more readily establishes infection of *N. benthamiana* [24].

A number of lines of evidence indicate that *CMPG1* activity may contribute to the necrotrophic phase of *P. infestans* infection. During this phase, transcript accumulation of *Avr3a* decreases markedly, potentially reducing the pathogen's capacity to stabilize *CMPG1* ([7]; Fig. S4). Conversely, at the onset of necrotrophy, both *INF1* and *CMPG1* transcripts were seen to accumulate co-ordinately, suggesting that necrotrophy may involve host PCD that is stimulated by the pathogen (Fig. S4). Consistent with this, the host cysteine protease cathepsin B, which is involved in PCD [25,26], is induced at a similar stage (3 dpi) of a compatible interaction between potato and *P. infestans* [27].

To further investigate the role of *CMPG1* in the necrotrophic phase, we silenced *CMPG1* in *N. benthamiana* and challenged silenced leaves with *P. infestans*. In TRV::*GFP* plants infection extended across the leaf, with massive sporulation by 6 dpi (Fig. 3C). In contrast, infection of plants inoculated with TRV::*NbCMPG1* showed significantly reduced sporulation (Fig. 3C 3E; Fig. S5) and lesion diameter (Fig. 3C, 3F), indicating that *NbCMPG1* activity positively impacts the late stages of *P. infestans* infection. *NbCMPG1* transcript levels were reduced in TRV::*NbCMPG1* plants to 25 % of the levels in control TRV::*GFP* plants (Fig. 3D).

Stabilization of *CMPG1* during infection indicates that it is a target for suppression of PTI. Nevertheless, remarkably, *CMPG1* activity is required for *P. infestans* during the late, necrotrophic phase of infection. A reasonable explanation is that host defenses which are

suppressed by a hemi-biotrophic pathogen at early stages of colonization, may be actively provoked to the pathogen's benefit at later stages. Although these results were unexpected, Arabidopsis RIN4, a widely studied target of bacterial effectors, is known to have contrasting functions as this protein both positively and negatively regulates plant immunity [28].

***Avr3a* is essential for virulence**

To investigate the contribution of AVR3a to virulence, isolate 88069 was transformed with constructs designed to stably silence *Avr3a*. A silenced line (CS12) was selected with *Avr3a* expression less than 5 % of wild-type levels. The silenced line grew and sporulated normally *in vitro*, but was significantly reduced in pathogenicity on susceptible potato cv Bintje (Fig. 4A), and on *N. benthamiana* (Fig. 4B; 4C).

We hypothesized that transient expression of *Avr3a* inside plant cells could complement the loss of virulence of CS12. Transient expression of *CFP-Avr3a^{KI}* in *N. benthamiana* led to detectable CFP fluorescence up to 5 days post-agroinfiltration (dpi), indicating that its expression was silenced by this time (Fig. S6). We thus surmised that if *P. infestans* was inoculated on the plants at 2 dpi, transient expression of *Avr3a* constructs in plant cells would persist for only the biotrophic phase of infection. Strikingly, transient expression of either *Avr3a^{EM}* (Fig. 4D; 4E) or *Avr3a^{KI}* in plant cells (Fig. 4F; 4G) restored virulence levels of CS12 to those of wild-type 88069 (Fig. 4H). In contrast, we observed no complementation of the *Avr3a*-silenced phenotype following transient expression of *Avr3a^{KI/Y147del}* (Fig. S7).

These results indicate that *Avr3a* is essential for virulence during the biotrophic phase. Moreover, they indicate that deletion of the terminal tyrosine from AVR3a^{KI}, although not effecting recognition by R3a, prevents either suppression of ICD or restoration of virulence to the AVR3a-silenced CS12 line.

Although little is known about the functions of eukaryote plant pathogen effectors, bacterial plant pathogen T3SS effectors suppress PTI and ETI by a number of enzymatic activities, through direct protein-protein interactions with defense-associated host targets [1-4]. The *Pseudomonas syringae* T3SS effector AvrPtoB exhibits ubiquitin E3 ligase activity which is required to suppress plant innate immunity, indicating that bacterial plant pathogens can modulate the host ubiquitin proteasome system (UPS) [29,30]. Oomycete plant pathogens translocate RXLR effector proteins into host cells to also promote susceptibility [7,9,10]. We

show that *P. infestans* RXLR effector AVR3a, which suppresses PCD triggered by the PAMP-like elicitor INF1 (ICD) [13,14], interacts with and stabilizes the host ubiquitin E3 ligase CMPG1, which is required for ICD [19]. An Avr3a^{KI/Y147del} mutant that lacks cell death suppression activity did not interact with or stabilize CMPG1. Stabilization of CMPG1 by AVR3a is thus consistent with the ability of this effector to suppress ICD by modifying CMPG1 activity, preventing the normal 26S proteasome-dependent degradation of itself, and thus potentially of its protein substrates in the host cell. In addition, we show that AVR3a, unlike many bacterial T3SS effectors, and despite the presence of hundreds of candidate RXLR effector genes in the *P. infestans* genome [31], is essential for virulence and thus functionally non-redundant. Critically, as the Avr3a^{KI/Y147del} mutant cannot suppress ICD, interact with or stabilize CMPG1, its failure to complement the AVR3a-silenced *P. infestans* line strongly implicates these activities in AVR3a's essential contribution to virulence. We report the first plant host target of a translocated effector from a filamentous eukaryotic plant pathogen, and show that this effector, like some bacterial effectors [32], is able to manipulate the host ubiquitin proteasome system to suppress plant immunity.

Materials and Methods

Microbial strains and growth conditions

A. tumefaciens strain GV3101 was used in molecular cloning experiments and was routinely cultured at 28°C in Luria-Bertani (LB) media using appropriate antibiotics [32]. *P. infestans* isolates Ca65 and 88069, and silenced line CS12, were maintained on rye sucrose agar plates as previously described [7].

Plasmid constructs

The constructs pGR106-FLAG-AVR3a^{KI} and FLAG-AVR3a^{EM} Δ23-147 were described previously [13], as was pGR106-AVR3a^{KI/Y147del} mutant (Δ23-146) with an N-terminal FLAG tag [14]. All additional Avr3a constructs for yeast-2-hybrid, for agroexpression *in planta*, and for fluorescent protein fusion, and all CMPG1 constructs for equivalent experiments, were cloned using the GATEWAY cloning system (Invitrogen, CA, USA), and details are given in Supplemental Data.

Yeast-2-hybrid screens

Yeast-2-hybrid screening was performed using the ProQuest™ system (Invitrogen) and details are given in Supplemental Data.

Agroinfiltration assays to investigate CMPG1 stabilization by western analyses

Recombinant *A. tumefaciens* strains were grown as described previously [33] except that the culturing steps were performed in LB media supplemented with 50 µg/mL of kanamycin. Agroinfiltration experiments were performed on 4-6 week-old *N. benthamiana* or *N. tabacum* plants as appropriate. Plants were grown and maintained throughout the experiments in a greenhouse with an ambient temperature of 22-25°C and high light intensity. Precise details of each agro-expression assay are provided in Supplemental Data.

INF1 protein infiltration

INF1 protein was produced in *Escherichia coli* carrying a pFLAG-ATS-INF1 expression construct as previously described [24]. Supernatants were infiltrated in RNAi stable transgenic tobacco and wild type tobacco in different dilutions (2x, 5x, 10x and 15x).

Western blot analyses

Samples for SDS-PAGE were prepared by grinding leaf tissue in liquid nitrogen followed by boiling for 5 minutes in SDS-loading buffer supplemented with 50µM DTT. The presence of recombinant myc-CMPG1 and FLAG-AVR3a *in planta* was determined by SDS-PAGE and Western blotting as described by Tian *et al.* [34]. For detection of CMPG1, western blots were incubated overnight with myc-antibodies diluted 1:4000 in PBS-T with 5% milk. Incubation with a secondary anti-rabbit HRP-conjugated antibody was performed for 1hr. Protein bands on western blots were detected using ECL substrate (Thermo Scientific Pierce). Additional western blot methods are described in Supplemental Data.

Confocal imaging

Nicotiana benthamiana plants were grown in a greenhouse at 22 °C (day temperature) and 18 °C (night temperature) with a minimum of 16 h light. *A. tumefaciens* transient expression was performed as described in Supplemental Data. Imaging was conducted on a Leica TCS-SP2 AOBS (Leica Microsystems Heidelberg GmbH, Germany) using HCX APO L 20x/0.5, 40x/0.8 and 63x/0.9 water dipping lenses as described in detail in Supplemental Data. PhotoshopCS software (Adobe Systems Incorporated, USA) was used for post-acquisition image processing. Quantification of fluorescence was performed using a SpectraMax M5 fluorimeter (Molecular Devices) as described in Supplemental Data.

Quantitative RT-PCRs

N. benthamiana leaves from 20 plants were sprayed with a *P. infestans* sporangia suspension of isolate 88069. 5 leaves were collected per day through a timecourse from 0 to 5 days. Sporangia cDNA from 88069 was prepared as described in [7]. Total RNA was extracted from the pooled leaf sample using RNeasy® Minikit (Qiagen). cDNA was synthesised from 3 µg of total RNA using random primers (Applied Biosystems) with SuperScript® II Reverse Transcriptase (Invitrogen) according to manufacturers instructions. cDNA was diluted by a factor of 10 and 2µl used per well with Power SYBR® Green PCR Master Mix (Applied Biosystems) in 25 µl reactions. Each PCR was performed in duplicate on a Chromo4 RT-PCR detector with DNA Engine® Peltier Thermal Cycler (Bio-Rad, Hemel Hempstead, UK) as described in Supplemental Data.

Transformation of *P. infestans*, silencing of *Avr3a*^{EM}, and testing silencing phenotype

The *PiAvr3a* gene was cloned as an inverted repeat, with the inverted copies separated by a 1422 bp intron (from AY310901) from the *Petunia hybrida* chalcone synthase (CS) gene as described in supplemental Data. Stable transformation of *P. infestans* isolate 88069 (homozygous *Avr3a*^{EM}) was achieved using a modified polyethylene glycol (PEG) – CaCl₂ – Lipofectin protocol (Supplemental Data). Modifications to this protocol were as described in Grouffaud *et al.* [35]. Sporangia were harvested from cultures of silenced transformant CS12 and wild type 88069 by flooding with sterile water, gentle rubbing with a glass rod, decanting of the solution, and centrifugation at 700 g for 5 min. Inoculation of detached *S. tuberosum* cv. Bintje leaves and

leaves of whole *N. benthamiana* plants was performed as described in Whisson *et al.* [7]. Complementation in *N. benthamiana* is described in detail in Supplemental Data.

Virus induced gene silencing (VIGS) of *NbCMPG1*

VIGS was performed using binary Tobacco Rattle Virus vectors in *N. benthamiana*. For *NbCMPG1* silencing, a 250bp fragment from within the equivalent region used for the *NtCMPG1* RNAi hairpin [6] was cloned in antisense as described in Supplemental Data. A TRV construct expressing GFP was used as a control as described in Gilroy *et al.* (2007) [25]. Analysis of VIGS in plants 3-4weeks post-inoculation with viruses by qRT-PCR, and *P. infestans* inoculations on VIGSed plants, are described in Supplemental Data.

Acknowledgement

We thank J. Jones for providing the CMPG1 RNAi tobacco lines, I. Malcuit and D. Baulcombe for providing the PVX vector, J. Lindbo for the pJL3-p19 vector, S. Schornack and E. Huitema for suggestions and comments on the manuscript. This work was supported by the Gatsby Charitable Foundation at TSL, by RERAD and BBSRC funding at the Universities of Dundee and Glasgow, and at SCRI.

References

1. Jones JD, Dangl, JL (2006) The plant immune system. *Nature* 444:323-329.
2. Chisholm ST, Coaker G, Day B, Staskawicz BJ (2006) Host-microbe interactions: shaping the evolution of the plant immune response. *Cell* 124:803-814.
3. Block A, Li G, Fu ZQ, Alfano JR (2008) Phytopathogen type III effector weaponry and their plant targets. *Curr Opin Plant Bio.* 11:396-403.
4. Grant SR, Fisher EJ, Chang JH, Mole BM, Dangl JL (2006) Subterfuge and manipulation: Type III effector proteins of phytopathogenic bacteria. *Ann Rev Microbiol* 60:425-449.
5. Kamoun S (2006) A Catalogue of the Effector Secretome of Plant Pathogenic Oomycetes. *Annu Rev Phytopathol* 44:41-60.
6. Kamoun S (2007) Groovy times: filamentous pathogen effectors revealed. *Curr Opin Plant Biol* 10:358-365.
7. Whisson SC, et al. (2007) A translocation signal for delivery of oomycete effector proteins into host plant cells. *Nature* 450:115- 119.
8. Birch PRJ, Rehmany AP, Pritchard L, Kamoun S, Beynon JL (2006) Trafficking arms: oomycete effectors enter host plant cells. *Trends in Microbiology* 14: 8-11.
9. Dou D, et al. (2008) RXLR-mediated entry of *Phytophthora sojae* effector *Avr1b* into soybean cells does not require pathogen-encoded machinery. *The Plant Cell* 20:1930-1947.

10. Birch PRJ, et al. (2008) Oomycete RXLR effectors: delivery, functional redundancy and durable disease resistance. *Curr Opin Plant Biol* 11:373-379.
11. Hein I, Gilroy EM, Armstrong MR, Birch PRJ (2009) The zig-zag-zig in oomycete-plant interactions. *Mol Plant Pathol* 10: 547-562.
12. Armstrong MR, et al. (2005) An ancestral oomycete locus contains late blight avirulence gene Avr3a, encoding a protein that is recognized in the host cytoplasm. *Proc Natl Acad Sci (USA)* 102:7766-7771.
13. Bos JIB, et al. (2006) The C-terminal half of *Phytophthora infestans* RXLR effector AVR3a is sufficient to trigger R3a-mediated hypersensitivity and suppress INF1-induced cell death in *Nicotiana benthamiana*. *Plant J* 48:165-176.
14. Bos JIB, Chaparro-Garcia A, Quesada-Ocampo LM, McSpadden Gardener BB, Kamoun S (2009) Distinct amino acids of the *Phytophthora infestans* effector AVR3a condition activation of R3a hypersensitivity and suppression of cell death. *Mol Plant-Microbe Interact* 22:269-281.
15. Vleeshouwers VGAA, et al. (2006) Agroinfection-based high-throughput screening reveals specific recognition of INF elicitors in *Solanum*. *Mol Plant Pathol* 7:499-510.
16. Hann DR, Rathjen JP (2007) Early events in the pathogenicity of *Pseudomonas syringae* on *Nicotiana benthamiana*. *Plant J* 49:607-618.
17. Kawamura Y, et al. (2009) INF1 elicitor activates jasmonic acid- and ethylene-mediated signalling pathways and induces resistance to bacterial wilt disease in tomato. *Journal of Phytopathology* 157:287-297.
18. Heese A, et al. (2007) The receptor-like kinase SERK3/BAK1 is a central regulator of innate immunity in plants. *Proc Natl Acad Sci (USA)* 104:12217-12222.
19. Gonzales-Lamothe R, et al. (2006) The U-box protein CMPG1 is required for efficient activation of defence mechanisms triggered by multiple resistance genes in tobacco and tomato. *The Plant Cell* 18:1067-1083.
20. Van der Hoorn RAL, Kamoun S (2008) From guard to decoy: a new model for perception of plant pathogen effectors. *The Plant Cell* 20:2009-2017.
21. Heise A, Lippok B, Kirsch C, Hahlbrock K (2002) Two immediate-early pathogen-responsive members of the *AtCMPG* family in *Arabidopsis thaliana* and the Wbox-containing elicitor-response element of *AtCMPG1*. *Proc Natl Acad Sci (USA)* 99:9049-9054.
22. Judelson HS, et al. (2008) Profiling the asexual development and pre-infection transcriptome of the late blight pathogen *Phytophthora infestans*. *Mol Plant-Microbe Interact* 21:433-447.
23. Kamoun S, et al. (1997) A gene encoding a protein elicitor of *Phytophthora infestans* is downregulated during infection of potato. *Mol Plant-Microbe Interact* 10:13-20.
24. Kamoun S, van West P, Vleeshouwers VGAA, de Groot KE, Govers F (1998) Resistance of *Nicotiana benthamiana* to *Phytophthora infestans* is mediated by the recognition of the elicitor protein INF1. *The Plant Cell* 10:1413-1425.
25. Gilroy EM, et al. (2007) Involvement of Cathepsin B in the Plant Disease Resistance Hypersensitive Response. *Plant J* 52:1-13.
26. McLellan H, Gilroy EM, Yun B-Y, Birch PRJ, Loake GJ (2009) Functional redundancy in the cathepsin B family contributes to basal and non-host resistance and senescence in *Arabidopsis thaliana*. *New Phytologist* 183:408-417.
27. Avrova AO, et al. (2004) Potato oxysterol binding protein and cathepsin B are rapidly up-

28. Mackey D, Belkhadir Y, Alonso JM, Ecker JR, Dangl JL (2003) Arabidopsis RIN4 is a target of the type III virulence effector AvrRpt2 and modulates RPS2-mediated resistance. *Cell* 112:379-389.
29. Abramovitch, R.B., Janjusevic, R., Stebbins, C.E., and Martin, G.B. (2006). Type III effector AvrPtoB requires intrinsic E3 ubiquitin ligase activity to suppress plant cell death and immunity. *Proc. Natl. Acad. Sci. (USA)*, 103:2851-2856.
30. Rosebrock, T.R., Zeng, L., Brady, J.J., Abramovitch, R.B., Xiao, F., Martin, G.B. (2007). A bacterial ubiquitin E3 ligase targets a host protein kinase to disrupt plant immunity. *Nature* 448: 370-374.
31. Haas BJ, et al. (2009) Genome sequence and analysis of the Irish potato famine pathogen *Phytophthora infestans*. *Nature* 461: 393-398.
32. Angot A, Vergunst A, Genin S, Peeters N (2007) Exploitation of the eukaryotic ubiquitin signaling pathways by effectors translocated by bacterial type III and type IV secretion systems. *PLoS Pathogens*, 3(1):e3.
33. Van der Hoorn RA, Laurent F, Roth R, De Wit PJ (2000) Agroinfiltration is a versatile tool that facilitates comparative analyses of Avr9/Cf-9-induced and Avr4/Cf-4- induced necrosis. *Mol Plant-Microbe Interact* 13:439-446.
34. Tian M, Huitema E, Da Cunha L, Torto-Alalibo T, Kamoun S (2004) A Kazalike extracellular serine protease inhibitor from *Phytophthora infestans* targets the tomato pathogenesis-related protease P69B. *J Biol Chem* 279:26370-26377.
35. Grouffaud S, van West P, Avrova AO, Birch PRJ, Whisson SC (2008) *Plasmodium falciparum* and *Hyaloperonospora parasitica* effector translocation motifs are functional in *Phytophthora infestans*. *Microbiology* 154:3743-51.

Figure Legends

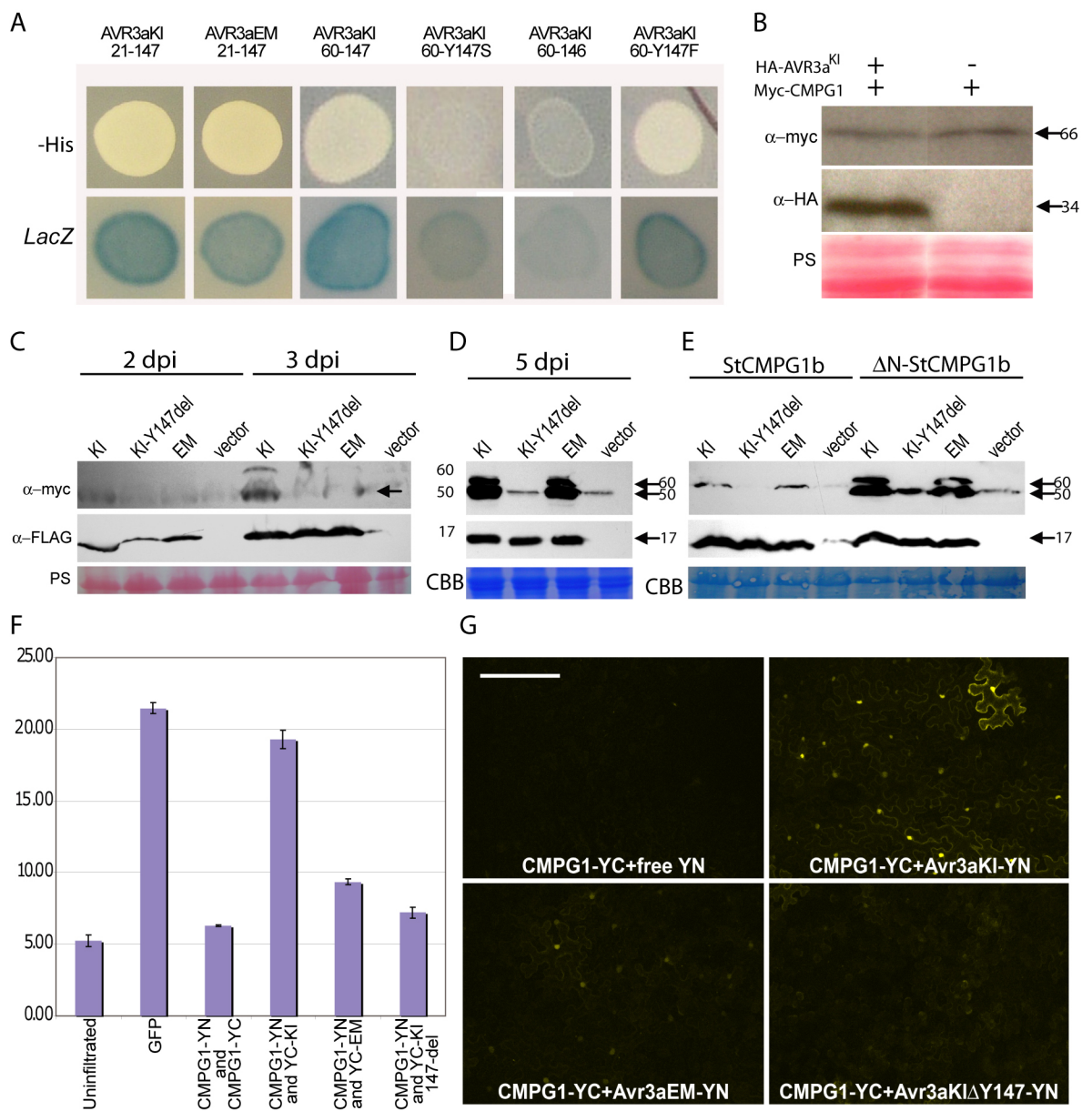
Fig. 1 AVR3a^{KI} and AVR3a^{EM} interact with and stabilize CMPG1. (A) AVR3a^{KI} and AVR3a^{EM} with (21-147) and without (60-147; shown only for AVR3a^{KI}) RXLR-encoding portions interact with CMPG1 in yeast-2-hybrid (LacZ and –His reporter genes activated). Whereas AVR3a^{KI/Y147del} (Y147 deletion) and AVR3a^{KI/Y147S} mutants fail to interact with CMPG1, the AVR3a^{KI/Y147F} mutant interacts. (B) Western blots probed with anti-myc and anti-HA antibodies following expression of mycCMPG1 in binding domain vector, with or without HA-AVR3a^{KI} in activation domain vector, in yeast. (C) Western blots probed with anti-myc and anti-FLAG antibodies, showing a time-course of transient co-expression (by agroinfiltration) of FLAG-AVR3a^{KI}, FLAG-AVR3a^{EM}, FLAG-AVR3a^{KI/Y147del} or a vector control with 4x-myc-ΔN-StCMPG1a at 2 and 3 days post-inoculation (dpi). (D) As in (C), but at 5 dpi. (E) as in (C) but at 5 dpi with 4x-myc-StCMPG1b (full-length) and 4x-myc-ΔN-StCMPG1b (lacking the N-terminal 29 amino acids). Protein sizes are indicated in kD. Protein loading is shown by coomassie blue (CBB) or Ponceau S staining (PS). (F) Fluorimeter measurements (in relative fluorescence units) following co-expression in *N. benthamiana* of the split YFP constructs CMPG1::N-YFP (YN), CMPG1::C-YFP (YC), C-YFP::AVR3a^{KI}, C-YFP::AVR3a^{EM}, C-YFP::AVR3a^{KI/Y147del} as indicated. (G) Confocal microscopy following co-expression in *N. benthamiana* of split YFP constructs CMPG1-YC with a vector expressing free N-YFP, and CMPG1-YC with N-

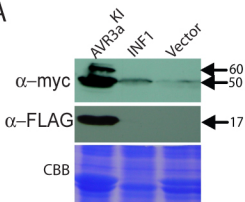
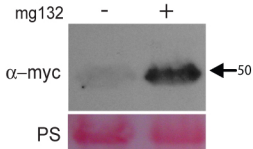
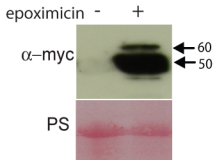
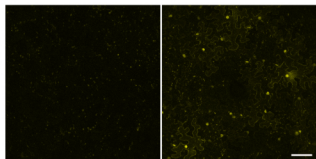
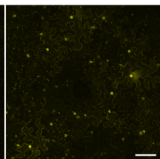
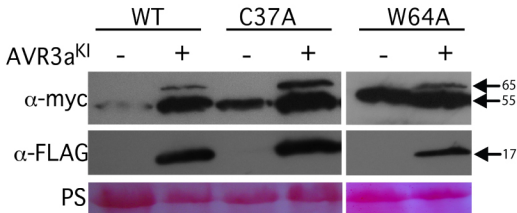
YFP::AVR3a^{KI}, N-YFP::AVR3a^{EM}, N-YFP::AVR3a^{KI/Y147del} constructs as indicated in the panels. Scale bars are 200 μ m.

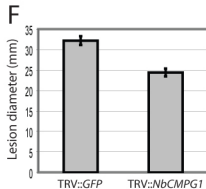
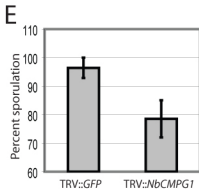
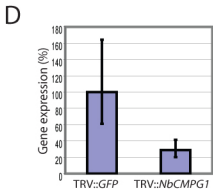
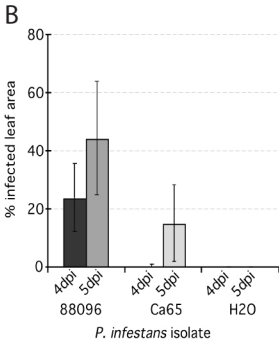
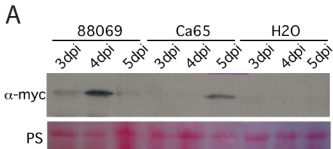
Fig. 2 CMPG1 stabilization is consistent with its inactivation or modification. (A) Western blot probed with anti-myc and anti-FLAG antibodies following co-expression of 4x-myc- Δ N-StCMPG1a with FLAG-AVR3a^{KI}, with INF1, or with empty vector control. (B) Western blots probed with anti-myc antibody, following expression of Δ N-4x-myc-StCMPG1a with or without MG132 inhibitor treatment as indicated. (C) Western blot probed as in (B) following expression of Δ N-4x-myc-StCMPG1a with or without epoxomicin inhibitor treatment. Confocal images of CMPG1-YFP following water (D) or epoxomicin (E) treatments. Scale bar (E) is 200 μ m. (F) Western blot probed as in (A) following expression of 4x-myc-NbCMPG1a, 4xmyc-NbCMPG1aC34A or 4x-myc-NbCMPG1aW64A with or without FLAG-AVR3a^{KI}. Sizes are indicated in kDa. Protein loading is shown by coomassie blue (CBB) or Ponceau staining (PS).

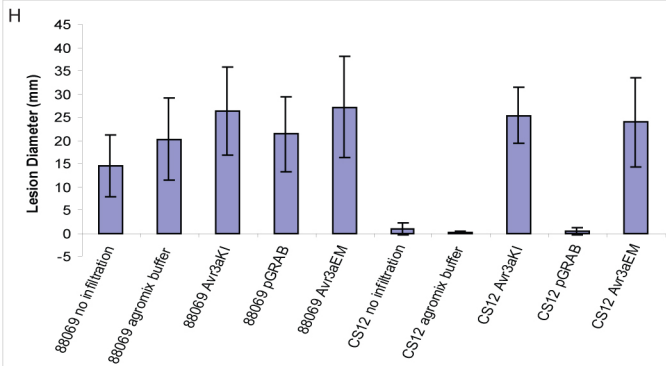
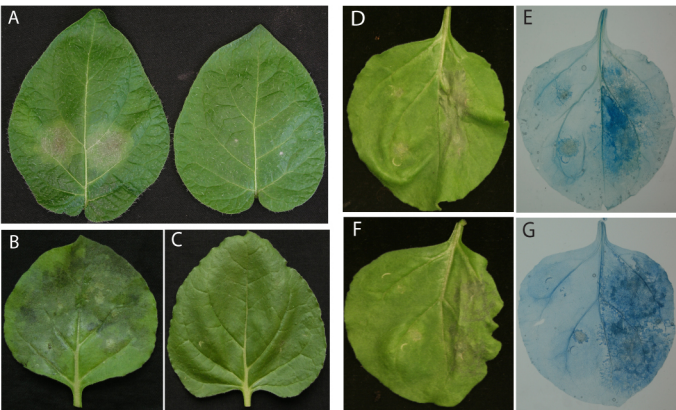
Fig. 3 CMPG1 is stabilized during infection. (A) Western blot probed with anti-myc antibody indicating stabilization of constitutively expressed Δ N-StCMPG1a-4x-myc across a time-course of *Nicotiana benthamiana* infection with *P. infestans* isolates 88069 and CA65. (B) Disease development, measured as % infected leaf area, of isolates 88069 and CA65 on *N. benthamiana* at 4 and 5 dpi. (C) Typical infection of *P. infestans* isolate 88069 on TRV::GFP-inoculated *N. benthamiana* (left leaf) and TRV::CMPG1-inoculated *N. benthamiana* (right leaf) at 6 dpi. (D) Real-time RT-PCR showing relative expression of *NbCMPG1* in *N. benthamiana* plants inoculated with TRV::GFP and TRV::CMPG1. (E) Percentage of *P. infestans* infection lesions that developed sporangia on TRV::GFP and TRV::CMPG1-inoculated *N. benthamiana* leaves at 6 dpi. (F) *P. infestans* infection lesion diameter (mm) TRV::GFP and TRV::CMPG1-inoculated *N. benthamiana* leaves at 6 dpi. VIGS experiments were repeated on 6 occasions with 6 replicate plants for each construct with reproducible results.

Fig. 4 *Avr3a* is essential for virulence. (A) Infection of potato cultivar Bintje by wild-type *Phytophthora infestans* isolate 88069 (left leaf) and *Avr3a*-silenced line CS12 (right leaf) at 4 days post-inoculation (dpi). (B) Infection of *N. benthamiana* by wild-type *P. infestans* isolate 88069 at 6 dpi. (C) Infection of *N. benthamiana* by *Avr3a*-silenced line CS12 at 6 dpi. (D) Infection of *N. benthamiana* by *Avr3a*-silenced line CS12 at 6 dpi, following agro-expression of pGRAB::*Avr3a*^{EM} (left half of leaf) or empty pGRAB (right half of leaf). (E) As in (D) but stained with trypan blue. (F) Infection of *N. benthamiana* by *Avr3a*-silenced line CS12 at 6 dpi, following agro-expression of pGRAB::*Avr3a*^{KI} (left half of leaf) or empty pGRAB (right half of leaf). (G) As in (F) but stained with trypan blue. (H) Measurements at 6 dpi of lesion sizes (mm) following infection of isolate 88069 or silenced line CS12 on leaves that were uninfiltrated, infiltrated with agromix, agro-infiltrated to express *AVR4a*^{KI}, *Avr3a*^{EM}, or empty pGRAB vector. These complementation experiments were repeated on 4 occasions, with leaves from 6 plants for each treatment/construct.



A**B****C****D****E****F**





Supporting Information

SI Material and Methods

Microbial strains and growth conditions

Agrobacterium tumefaciens strains GV3101 and AGL1 were used in molecular cloning and transient expression experiments and routinely cultured at 28°C in Luria-Bertani (LB) or yeast extract broth (YEB) media using appropriate antibiotics (1). All *A. tumefaciens* DNA transformations were conducted by electroporation (1). *P. infestans* isolates Ca65 and 88069, and silenced line CS12, were maintained on rye sucrose agar plates as previously described (2).

Plasmid constructs

The constructs pGR106-FLAG-AVR3a^{KI} and FLAG-AVR3a^{EM} Δ23-147 were described previously (3), as was pGR106-AVR3a^{KI/Y147del} mutant (Δ23-146) with an N-terminal FLAG tag (4).

We generated GATEWAY ENTRY vector constructs for both alleles of AVR3a using the 5' primer 5'AAGGGGATCCCCATCGACCAAACCAAGGTC 3' which contains a *Bam*HI site and anneals after the 21 amino acid signal peptide. This primer was used in combination with the 3' primer 5'AAGGGAATTCTTATATCCAGTGAGCCC 3' which contains a *Eco*RI site. We amplified both alleles from existing AVR3a constructs using high fidelity PCR, digested with *Bam*HI and *Eco*RI, and ligated into pENTR1A to generate pENTR1A-AVR3a^{KI} and pENTR1A-AVR3a^{EM}. We generated AVR3a effector domain constructs using the 5' primer 5'AAGGGGATCCGAGCCCCAAATTTCAATTTG 3' which contains a *Bam*HI site and anneals after the 60th amino acid of the AVR3a sequence and thus removes the RXLR translocation domain. This primer was used in combination with the following 3' primers all of which contain *Eco*RI sites; 5' AAGGGAATTCTAAAATCCAGTGAGCCCCAG 3' which replaces the terminal TAT Tyrosine codon with TTT Phenylalanine to generate pENTR1A-AVR3aCF-F147R, 5' AAGGGAATTCTAAGA TCCAGTGAGCCCCAG 3' which replaces the terminal TAT codon with TCT Serine to generate pENTR1A-AVR3aCF-S147R, 5' AAGGGAATTCTATCCAGTGAGCCCCAGGTG 3' which removes the terminal codon entirely and generates pENTR1A-AVR3aCF-Δ147R. Combining this 5' primer with the original 3' primer generated the wild type AVR3a effector domain construct pENTR1A-AVR3aCF-Y147R. We amplified the AVR3a effector domain using these primers and high fidelity PCR using pENTR1A-AVR3a^{KI} as template, before digestion and ligation into pENTR1A as before.

We generated the *StCMPG1b* constructs using the GATEWAY cloning system (Invitrogen, CA, USA). The 5' CMPG1 primer 5' GGATCCTAGAGATGATTGCAACATGGAGAA 3' was based on the Avr9/Cf-9 rapidly elicited protein from *Solanum lycopersicum* (tomato) protein sequence accession number Q1WM08 as the amino-terminal approximately 30 amino acid residues of the *S. tuberosum* sequence (Δ*N-StCMPG1a*) in the Y2H library clones were absent but the amino-terminal sequences of the tomato and tobacco homologues and the remainder of the potato sequence was highly conserved (alignment in Figure S1). A *Bam*HI site was added to the 5' primer for cloning into pENTR1A (Invitrogen). The 3' CMPG1 primer 5' CGGCCGCTTTCCAAATGTCCTTTTGAGACTCTTGA 3' was designed to the Δ*N-StCMPG1a* sequence recovered from the yeast-2-hybrid library, the stop codon was changed to a glycine codon to allow C-terminal fusions and an *Eag*I site was added for cloning. To generate the N-

terminal truncated version of *StCMPG1b* we PCR-amplified, using the full length construct as template, with primers CMPG1_sh_F: ‘CACCATGGAGTTAGTGATACCA ATCCAATTTAC and CMPG1-R1: TCAAAATGTCCTTTTGAGACTCTTG. We amplified full-length *NbCMPG1* sequences from *N. benthamiana* genomic DNA using the primers NtCMPG1-F-ENTR: 5’-CACCATGATTTC AACATGGAGGAAAAG -3’ and NtCMPG1-R-ENTR: CTATCAGAATGGCCTTTTGAGACTCTT. The full-length tomato (VF36) *SICMPG1* was amplified from genomic DNA with the primers SICMPG1-F-ENTR : 5’ CACCATGATTGCAACATGGAGAAAAAAGAG-3’ and CMPG1-R1. The NbCMPG1a C37A and NbCMPG1a W64A mutants were generated by overlap extension PCR using primers NtCMPG1-F-ENTR with CMPG-C37A-R: 5’-TCTAAGGAAATTGGAGCTGTGAAATGTCTAGGAATCACCAACTCC-3’ and NtCMPG1-R-ENTR with CMPG-C37A-F: 5’-GGAGTTGGTGATTCCCTAGACATTTACAGCTCCAATTTCTTAGA-3’ for the NbCMPG1a C37A mutant and NtCMPG1-F-ENTR with CMPGW64A-R: 5’-GTTTGATTCCCAGCCTCAATCGCTTTCTCAATATTCTCTATCGT-3’ and NtCMPG1-R-ENTR with CMPGW64A-F: 5’-ACGATAGAGAGAATATTGAGAAAGCGATTGAGGCTGGGAATCAAAC-3’ for the NbCMPG1a W64A mutant. For each mutant, amplicons were mixed in a 1:1 ratio and used as template for a second round of PCR with primers NtCMPG1-F-ENTR and NtCMP1-R-ENTR. Amplicons were cloned in the pENTR-TOPO vector according to manufacturer’s recommendations (Invitrogen, CA, USA). Entry vector constructs were sequenced and used for LR recombination reactions with the plant expression vector pGWB18 to generate N-terminal 4xmyc fusions.

Fluorescent protein (FP) fusions were generated using the Gateway® LR clonase® enzyme mix (Invitrogen) to recombine the entry vector clones of Avr3a and CMPG1 with plant expression vectors. The vectors pB7YWG2 and pB7WGC2 were used for fusions to YFP and CFP, respectively (5). pBAT-TL-B-sYFP-N, pBAT-TL-B-sYFP-C (6) and two home-made variants of these (pCL112 and 113) were used to create split YFP fusions (YN or YC) for bimolecular fluorescence complementation (7). For expression of an untagged Avr3a to use in combination with the fluorescent protein fusions pENTR1A-AVR3aCF-Y147R was recombined with pEarleyGate203 (8).

Summary of GATEWAY recombination constructs for fluorescent protein fusions

FP fusion	Source clone for recombination	Destination vector	Notes
CFP::Avr3a ^{KI}	pENTR1A.Avr3a ^{KI}	pB7WGC2	Δsignal peptide
CFP::Avr3a ^{EM}	pENTR1A.Avr3a ^{EM}	pB7WGC2	Δsignal peptide
CFP::Avr3a ^{KI/Y147-del}	pENTR1A.Avr3a ^{KI/Y147-del} 1.4	pB7WGC2	Δsignal peptide
C-YFP::Avr3a ^{KI}	pENTR1A.CFY147R (<i>AVR3a^{KI}</i>)	pCL113	Δsignal peptide ΔRXLR
N-YFP::Avr3a ^{KI}	pENTR1A.CFY147R (<i>AVR3a^{KI}</i>)	pCL112	Δsignal peptide

			ΔRXLR
N-YFP::Avr3a ^{EM}	pENTR1A. Avr3a ^{EM} 1.1	pCL112	Δsignal peptide ΔRXLR
C-YFP::Avr3a ^{EM}	pENTR1A. Avr3a ^{EM} 1.1	pCL113	Δsignal peptide ΔRXLR
C-YFP::Avr3a ^{KI/Y147-del}	pENTR1A.CFΔ147R (Avr3a ^{KI/Y147-del})	pCL113	Δsignal peptide ΔRXLR
N-YFP::Avr3a ^{KI/Y147-del}	pENTR1A.CFΔ147R (Avr3a ^{KI/Y147-del})	pCL112	Δsignal peptide ΔRXLR
StCMPG1b::C-YFP	pENTR1A.StCMPG1b	pBatTL-B-sYFPC	
StCMPG1b::N-YFP	pENTR1A.StCMPG1b	pBatTL-B-sYFPN	
StCMPG1b::YFP	pENTR1A.StCMPG1b	pB7YWG2	

Yeast-2-hybrid screens

Yeast-2-hybrid screening was performed using the ProQuest™ system (Invitrogen). Briefly, DNA binding domain "bait" fusions were generated by recombination between either pENTR1A-AVR3a^{KI} or pENTR1A-AVR3a^{EM} and pDEST32, generating pEXP32-AVR3a^{KI} or pEXP32-AVR3a^{EM}. These constructs were transformed into yeast strain MaV203 and nutritional selection used to recover transformants. A single transformant from each transformation was then grown up and used to prepare competent yeast cells which were then transformed with a potato yeast-2-hybrid library commercially prepared from infected leaf material 15 and 72 hours post inoculation. Approximately 10 million co-transformants were screened with either allele. Observed interactors were confirmed by re-transformation with the bait construct or with the empty bait vector to rule out the possibility of interactions between the prey and the DNA binding domain of the bait construct, or DNA binding activity of the prey itself.

Agroinfiltrations to investigate CMPG1 stabilization by western analyses

Recombinant *A. tumefaciens* strains were grown as described previously (9) except that the culturing steps were performed in LB media supplemented with 50 ug/mL of kanamycin. Agroinfiltration experiments were performed on 4-6 week-old *N. benthamiana* plants. Plants were grown and maintained throughout the experiments in a greenhouse with an ambient temperature of 22°-25°C and high light intensity.

Transient co-expression of 35S-R3a and pGR106-FLAG-AVR3a^{KI}, AVR3a^{EM} and Avr3a^{KI/Y147-del} in CMPG1 RNAi stable transgenic (10) and wild-type tobacco was performed as follows: *A. tumefaciens* strains carrying the respective constructs were mixed in a 2:1 ratio in

induction buffer to a final optical density at 600 nm (OD_{600}) of 0.4. Symptom development was monitored from 3-8 days after infiltration.

To assays for INF1 cell death in CMPG1 silenced tobacco, INF1 protein was produced in *Escherichia coli* carrying a pFLAG-ATS-INF1 expression construct as previously described (11). Supernatants were infiltrated in RNAi stable transgenic tobacco and wild type tobacco in different dilutions (2x, 5x, 10x and 15x).

For western blot analyses of leaves co-expressing pGWB18-CMPG1 and pGR106-FLAG-AVR3a^{KI}, AVR3a^{EM} ($\Delta 23-147$), Avr3a^{KI/Y147-del} ($\Delta 23-146$) or vector control, agroinfiltration was performed with a mix of *Agrobacterium* strains expressing the respective constructs in combination with a strain containing pJL3-p19 (obtained from J. Lindbo), a binary vector that expresses the suppressor of post-transcriptional gene silencing p19 of *Tomato bushy stunt virus* (TBSV) (12). For each of the *Agrobacterium* strains a final OD_{600} of 0.3 in induction buffer was used. All four different *Agrobacterium* mixes (i.e. with AVR3a^{KI}, Avr3a^{KI/Y147-del}, AVR3a^{EM} or vector control) were infiltrated on the same leaf. Infiltration sites from 4 different leaves were harvested and pooled for western blot analyses.

To perform western blot analyses of CMPG1 during *P. infestans* infection, whole *N. benthamiana* leaves were agroinfiltrated with a combination of *Agrobacterium* strains expressing ΔN -StCMPG1a and p19. For both *Agrobacterium* strains a final OD_{600} of 0.3 in induction buffer was used. Leaves were challenged 1 dpi with zoospores of *P. infestans*, by dipping the underside of leaves in a zoospore solution (of isolates CA65 or 88069) of 50,000 zoospores/mL. Infection assays were performed on detached leaves as described previously (13).

For comparing stabilization of CMPG1 by MG132 and AVR3a by western blot analyses, we agroinfiltrated strains expressing the pGWB18-CMPG1 construct in combination with pGR106-FLAG-AVR3a^{KI} or pGR106- Δ GFP and pJL3-p19 as described above. Three days later, infiltration sites were challenged with 100uM MG132 (Sigma Aldrich) in 1% DMSO and 1% DMSO alone as a control, or with 50uM epoxomicin (Calbiochem) in 5% DMSO and 5% DMSO alone as a control. Leaf discs were harvested 16 hours after MG132 infiltration.

For assessing the stabilization of CMPG1 during INF1-mediated cell death, leaves of *N. benthamiana* were infiltrated with *Agrobacterium* strains carrying pGWB18-CMPG1 in combination with pJL3-19 as described above. As a control for stabilization, we co-expressed pGWB18-CMPG1 with pGR106-FLAG-AVR3a^{KI} as described above. One day later, infiltration sites expressing only CMPG1 were challenge infiltrated with *Agrobacterium* strains carrying p35S-INF1 or p35S-vector at and OD_{600} of 0.3. Leaf discs were harvested 2 days after infiltration of p35S-INF1. For assessing CMPG1-YFP stability during INF1 cell death, *Agrobacterium* strains carrying StCMPG1b-YFP and p35S-INF1 (4) were co-infiltrated at a final OD_{600} of 0.1 and imaged over 3 days as described below.

Western blot analyses

Samples for SDS-PAGE were prepared by grinding leaf tissue in liquid nitrogen followed by boiling for 5 minutes in SDS-loading buffer supplemented with 50uM DTT. The presence of recombinant myc-CMPG1 and FLAG-AVR3a was determined by SDS-PAGE and Western blotting as described previously (14). To detect myc-CMPG1 in yeast we used Anti-Myc-HRP antibody from (Invitrogen), and for detection of HA-AVR3a^{KI} we used anti-HA from Mouse (Invitrogen), followed by anti-Mouse-HRP from Goat (Sigma). Monoclonal FLAG M2

antibodies and polyclonal myc-antibodies (sc-789) were obtained from Sigma (St. Louis, MO) and Santa Cruz Biotechnology Inc. (Santa Cruz, CA) respectively. Polyclonal GFP antibody obtained from Invitrogen (A-6455) was used to detect recombinant CFP-AVR3a variants

Confocal imaging

Nicotiana benthamiana plants were grown in a greenhouse at 22 °C (day temperature) and 18 °C (night temperature) with a minimum of 16 h light. *A. tumefaciens* transient expression was performed largely as described previously (2005). In brief, overnight *Agrobacterium* cultures were centrifuged, the pellets resuspended in infiltration buffer (10 mM MgCl₂, 10 mM MES pH 5.6, 15 µM acetosyringone) and the concentrations measured as OD₆₀₀. The bacterial suspension was diluted with the same buffer to adjust the inoculum concentration to final OD₆₀₀ values of between 0.01 and 0.1 depending on the experiment. Infiltrations were performed with a needleless syringe as described previously (16). For experiments requiring co-infiltration of more than one construct, bacterial strains containing the constructs were mixed prior to the leaf infiltration, with the concentration of each strain adjusted to the required final OD₆₀₀. Where required the infiltrated area of the leaf was delimited and labelled with a fine-tip indelible pen. Infiltrated plants were incubated under normal growth conditions as above. To assay stabilization of StCMPG1b::YFP by epoxomicin we agroinfiltrated the strain expressing the fusion and three days later, re-infiltrated the sites with 50µM epoxomicin (Sigma Aldrich) in 5% methanol or 5% methanol alone as a control. Leaves were imaged 24 hours after epoxomicin infiltration.

Imaging was conducted on a Leica TCS-SP2 AOBS (Leica Microsystems Heidelberg GmbH, Germany) using HCX APO L 20x/0.5, 40x/0.8 and 63x/0.9 water dipping lenses. CFP was imaged using 405 nm excitation and its emission was collected from 455–480 nm. The excitation wavelength for YFP was 514 nm and its emission was collected from 525–580 nm when co-expressed with CFP and 530–575 nm when expressed alone or as split-YFP. Co-expressed CFP and YFP were imaged sequentially using a line by line mode. The optimal pinhole diameter was maintained at all times. PhotoshopCS software (Adobe Systems Incorporated, USA) was used for post-acquisition image processing.

Quantification of fluorescence was performed using a SpectraMax M5 fluorimeter (Molecular Devices). Leaf tissue was ground in phosphate buffered saline (PBS) containing protease inhibitor cocktail (Complete, Roche) centrifuged to clear the grindate. YFP fluorescence was excited at 514 nm and measured at 580 nm.

Quantitative RT-PCRs

N. benthamiana leaves from 20 plants were sprayed with a *P. infestans* sporangia suspension of isolate 88069. 5 leaves were collected per day through a timecourse from 0 to 5 days. Sporangia cDNA from 88069 was prepared as described previously (2). Total RNA was extracted from the pooled leaf sample using RNeasy® Minikit (Qiagen). cDNA was synthesised from 3 µg of total RNA using random primers (Applied Biosystems) with SuperScript® II Reverse Transcriptase (Invitrogen) according to manufacturers instructions. cDNA was diluted by a factor of 10 and 2µl used per well with Power SYBR® Green PCR Master Mix (Applied Biosystems) in 25 µl reactions. Each PCR was performed in duplicate on a Chromo4 RT-PCR detector with DNA Engine® Peltier Thermal Cycler (Bio-Rad, Hemel Hempstead, UK). Primers for genes are as follows: *Nb25S*, 5'-CACGGACCAAGGAGTCTGACAT-3' and 5'-TCCCACCAATCAGCTTCCTTAC-3' *NbCMPG1* 5'-GTGTGCCTGTTTTGGTGAAG-3' and 5'-TTTTGAAATGCACCAACTTGA-3' *PiActA* 5'-CATCAAGGAGAAGCTGACGTACA-

3' and 5'-GACGACTCGGCGGCAG-3' *PiAvr3a* 5'-CGCCATAAACTTTGCAACCA-3' and 5'-TGCCGGCTGAATCGTGTAT-3' *PiCdc14*, 5'-TGCACTTTTAACTTGACTATTCTTGA-3' and 5'-AGATCAAACGTCTTAGTGGAGATG-3' *PiInfl* 5'-GTCTACGTGTGCGTCGCTAT-3' and 5'-CGGAGAACAAAGCCTAATCG-3'. PCR parameters were as follows: 95°C, 15min; 95°C, 15s; 59°C, 30s; 72°C, 30s (40 cycles). Melting curve analyses were performed on every run to confirm single product (58°C to 95°C) reading every 1°C. *P. infestans* gene expression cT values were normalised with Actin and made relative to sporangia. *NbCMPGI* cT values were normalised with 25S expression and made relative to GFP (for VIGS) control or day 0 (for expression during infection).

Transformation of *P. infestans*, silencing of *Avr3a*^{EM}, and testing silencing phenotype

The *PiAvr3a* gene was cloned as an inverted repeat, with the inverted copies separated by a 1422 bp intron (from AY310901) from the *Petunia hybrida* chalcone synthase (CS) gene. The CS intron was PCR amplified using primers CHAL_SYN_INT_EcoF (ggaagaattctttaaattgtgaagaattcttattgt) and CHAL_SYN_INT_XbaR (ggaatctagatccaaatactgcaaatgacca). Each 50 µl PCR reaction contained the following components: 0.5 U Phusion Hot Start DNA polymerase (New England Biolabs), 10 µl of 5 × reaction buffer (New England BioLabs), 15 mM dNTPs (Promega), 30 µM forward and reverse primers, and 10 ng CS intron plasmid DNA. Thermocycling conditions used an initial melt of 98 °C for 2 min, followed by 35 cycles of 98 °C for 10 s, 60 °C for 30 s, and 72 °C for 1 min. A final extension step of 72 °C for 10 min was included. PCR products were purified (QIAGEN Minelute kit), digested with EcoRI and XbaI restriction endonucleases (Promega, UK), and purified again by Minelute. PCR products were directionally ligated, using T4 DNA ligase (Promega, UK), into the EcoRI and XbaI sites of vector pTor (17) for constitutive overexpression from the *Bremia lactucae* *Ham34* promoter. The *Avr3a* gene was PCR amplified using the same conditions using primer pairs *Avr3a*ClaF2 (5'-GGAAATCGATACCATGCGTCTGGCAATTATGCTG-3') and *Avr3a*EcoRIR (5'-GGAAGAATTCTCCAGAGAGCCCCAGGTGCAT-3'), and *Avr3a*SacF (5'-GGAACCGCGGACCATGCGTCTGGCAATTATGCT-3') and *Avr3a*XbaR (5'-GGAATCTAGATCCAGAGAGCCCCAGGTGCAT-3'). PCR products were purified and digested (*Cla*I and *Eco*RI for sense; *Xba*I and *Sac*II for antisense) as described, then cloned into the *Cla*I and *Eco*RI sites, and into the *Xba*I and *Sac*II sites of the pTor vector containing the CS intron. Insert orientation and integrity was confirmed by DNA sequencing. Stable transformation of *P. infestans* isolate 88069 (homozygous *avr3a*^{EM}) was achieved using a modified polyethylene glycol (PEG) – CaCl₂ – Lipofectin protocol (18); <http://138.23.152.128/protocols/protocols.html>). Modifications to this protocol were as described previously (19).

Sporangia were harvested from cultures of silenced transformant CS12 and wild type 88069 by flooding with sterile water, gentle rubbing with a glass rod, decanting of the solution, and centrifugation at 700 g for 5 min. Inoculation of detached *S. tuberosum* cv. Bintje leaves and leaves of whole *N. benthamiana* plants was performed as described previously (2). Complementation in *N. benthamiana* was achieved by agroinfiltrating approximately 4 week old plants with respective control and *Avr3a* construct at an OD₆₀₀ of 0.5 two days prior to *P. infestans* inoculation. The oldest and youngest *N. benthamiana* leaves were avoided. For *N. benthamiana* leaves that had been agroinfiltrated with *Avr3a* alleles, there were four sites of *P. infestans* inoculation per leaf, at the centre of each infiltration site. Lesion sizes were recorded at

7 days post inoculation (dpi), mean lesion size and standard deviation calculated. Biological replicate experiments were performed with technical replication with each biological replicate. Inoculated leaves were photographed at 7 dpi using an Olympus Camedia C-5050 digital camera under natural light. Trypan blue staining was performed as described previously (20) and pictures taken through a white light source.

Virus induced gene silencing (VIGS) of *NbCMPGI*

VIGS was performed as described in Peart et al., (2002), using binary Tobacco Rattle Virus vectors in *Nicotiana benthamiana*. For *NbCMPGI* silencing, a 250bp fragment from within the equivalent region used for the *NiCMPGI* RNAi hairpin (9) was cloned in antisense, using the following primers: 5'-AAAAGAATTCAAGGAAAATGATCCAACAATGG-3' and 5'-AAAAGTTAACTGCAACAAATGCAGCTGATAA-3'. A TRV construct expressing GFP was used as a control as described previously (20). VIGS was analysed in plants 3-4 weeks post-inoculation with viruses by qRT-PCR. A pool of two leaves from 6 plants for each construct was used for RNA extractions and cDNA was synthesised as described above. VIGSed plants were inoculated with *P. infestans* and lesion sizes were assessed as described above (transformation and silencing of *AVR3a*). 10 µl of concentrated spore suspension was pipetted on 4 independent regions of each leaf. The middle leaves from each VIGSed plant were used and the experiments were repeated 4 times.

1. Sambrook, J. and Russell, D.W. (2001). Molecular Cloning. (Cold Spring Harbor Laboratory Press, Cold Spring Harbor, New York, USA).
2. Whisson, S.C., Boevink, P.C., Moleleki, L., Avrova, A.O., Morales, J.G., Gilroy, E.M., Armstrong, M.R., Grouffaud, S., van West, P., Chapman, S. *et al.* (2007) A translocation signal for delivery of oomycete effector proteins into host plant cells. *Nature*, 450, 115-119.
3. Bos JIB, et al. (2006) The C-terminal half of *Phytophthora infestans* RXLR effector AVR3a is sufficient to trigger R3a-mediated hypersensitivity and suppress INF1-induced cell death in *Nicotiana benthamiana*. *Plant J* 48:165-176.
4. Bos, J.I.B., Chaparro-Garcia, A., Quesada-Ocampo, L.M., McSpadden Gardener, B.B., and Kamoun, S. (2009). Distinct amino acids of the *Phytophthora infestans* effector AVR3a condition activation of R3a hypersensitivity and suppression of cell death. *Mol. Plant-Microbe Interact.*, 22, 269-281.
5. Karimi, M., De Meyer, B. and Hilson, P. (2005) Modular cloning and expression of tagged fluorescent protein in plant cells. *Trends Plant Sci.* 10(3): 103-105.
6. Uhrig JF, Mutondo M, Zimmermann I, Deeks MJ, Machesky LM, Thomas P, Uhrig S, Rambke C, Hussey PJ, Hülskamp M (2007) The role of Arabidopsis SCAR genes in ARP2-ARP3-dependent cell morphogenesis. *Development* 134, 967-977.
7. Bracha-Drori, K., Shichrur, A. Katz, M. Oliva, R. Angelovici, S. Yalovsky, and N. Ohad. (2004) Detection of protein-protein interactions in plants using bimolecular fluorescence complementation. *Plant J.* 40:419-427.
8. Earley K, Haag JR, Pontes O, Opper K, Juehne T, Song K, and Pikaard CS (2006). Gateway-compatible vectors for plant functional genomics and proteomics. *The Plant J.* 45:616-629.

9. Van der Hoorn, R.A., Laurent, F., Roth, R., and De Wit, P.J. (2000). Agroinfiltration is a versatile tool that facilitates comparative analyses of Avr9/Cf-9-induced and Avr4/Cf-4-induced necrosis. *Mol. Plant-Microbe Interact.*, 13, 439-446.
10. Gonzàles-Lamothe, R., Tsitsigiannis, D.I., Ludwig, A.A., Panicot, M., Shirasu, K., and Jones, J.D.G. (2006). The U-box protein CMPG1 is required for efficient activation of defence mechanisms triggered by multiple resistance genes in tobacco and tomato. *The Plant Cell*, 18, 1067-1083.
11. Kamoun S, van West P, Vleeshouwers VGAA, de Groot KE, Govers F (1998) Resistance of *Nicotiana benthamiana* to *Phytophthora infestans* is mediated by the recognition of the elicitor protein INF1. *The Plant Cell* 10:1413-1425.
12. Voinnet O, Rivas S, Mestre P, Baulcombe D (2003) An enhanced transient expression system in plants based on suppression of gene silencing by the p19 protein of tomato bushy stunt virus. *Plant J* 33, 949-956.
13. Vleeshouwers VGAA, van Doijeweert, Govers F, Kamoun S, Colon LT (2000) The hypersensitive response is associated with host and non-host resistance to *Phytophthora infestans*. *Planta* 210, 853-864.
14. Tian M, Huitema E, Da Cunha L, Torto-Alalibo T, Kamoun S (2004) A Kazal-like extracellular serine protease inhibitor from *Phytophthora infestans* targets the tomato pathogenesis-related protease P69B. *J Biol Chem* 279:26370-26377.
15. Latijnhouwers M, Hawes C, Carvalho C, Oparka K, Gillingham AK, Boevink P. An Arabidopsis GRIP domain protein locates to the trans-Golgi and binds the small GTPase ARL1. *Plant J.* (2005) 44:459–470.
16. Batoko H, Zheng HQ, Hawes C, Moore I. A Rab1 GTPase is required for transport between the endoplasmic reticulum and Golgi apparatus and for normal Golgi movement in plants. *Plant Cell* (2000) 12:2201–2218.
17. Blanco, F. A., and Judelson, H. S. (2005) A bZIP transcription factor from *Phytophthora* interacts with a protein kinase and is required for zoospore motility and plant infection. *Molecular Microbiology* 56, 638-648.
18. Judelson, H. S., Tyler, B.M., and Michelmore, R.W. (1991) Stable transformation of the oomycete pathogen, *Phytophthora infestans*. *Molecular Plant-Microbe Interactions*. 4, 602-607.
19. Grouffaud, S., van West, P., Avrova, A.O., Birch, P.R.J. and Whisson, S.C. (2008) *Plasmodium falciparum* and *Hyaloperonospora parasitica* effector translocation motifs are functional in *Phytophthora infestans*. *Microbiology*, 154, 3743-3751.
20. Gilroy EM, Hein I, van der Hoorn R, Boevink PC, Venter E, McLellan H, Kaffarnik F, Pritchard L, Hrubikova K, Shaw J, Holeva M, Loake GJ, Lacomme C, Birch PRJ (2007). Involvement of Cathepsin B in the Plant Disease Resistance Hypersensitive Response. *Plant J*, 52, 1-13.

Table S1: Candidate AVR3a-interacting proteins (PI) identified in yeast-2-hybrid analyses

ID	Best BLASTP match	Score	E value	Interpro Domains
AVR3aPI-1	ref XP_002270689.1 PREDICTED: similar to pyruvate kinase family protein [Vitis vinifera]	868	0.0	Pyruvate/Phosphoenolpyruvate kinase, catalytic core (InterPro:IPR015813), Pyruvate kinase, beta-barrel-like (InterPro:IPR011037), Pyruvate kinase (InterPro:IPR001697), Pyruvate kinase, barrel (InterPro:IPR015793)
AVR3aPI-2	ref XP_002269327.1 PREDICTED: hypothetical protein [Vitis vinifera]	390	9e-107	
AVR3aPI-3 (CMPG1)	ref XP_002281552.1 PREDICTED: hypothetical protein [Vitis vinifera]	483	1e-134	U box (InterPro:IPR003613) Armadillo-like helical (InterPro:IPR011989) Armadillo-type fold (InterPro:IPR016024)
AVR3aPI-4	ref XP_002269025.1 PREDICTED: hypothetical protein [Vitis vinifera]	1640	0.0	
AVR3aPI-5	ref XP_002262721.1 PREDICTED: hypothetical protein [Vitis vinifera]	480	4e-148	Acyl-ACP thioesterase (InterPro:IPR002864)
AVR3aPI-6	ref XP_002513805.1 heat shock protein 70 (HSP70)-interacting protein, putative [Ricinus communis]	448	5e-124	Tetratricopeptide TPR-1 (InterPro:IPR001440), Tetratricopeptide-like helical (InterPro:IPR011990), Tetratricopeptide region (InterPro:IPR013026)
AVR3aPI-7	ref XP_002510325.1 exocyst complex component sec3, putative [Ricinus communis]	1516	0.0	Exocyst complex, component Exoc1 (Sec3) (InterPro:IPR019160)
AVR3aPI-8	ref XP_002265426.1 PREDICTED: hypothetical protein [Vitis vinifera]	706	0.0	
AVR3aPI-9	ref XP_002532309.1 conserved hypothetical protein [Ricinus communis]	372	4e-101	
AVR3aPI-10	ref XP_002264216.1 PREDICTED: hypothetical protein [Vitis vinifera]	1387	0.0	DEAD-like helicase, N-terminal (InterPro:IPR014001) ATPase_AAA+_core (InterPro:IPR003593)
AVR3aPI-11	ref XP_002274797.1 PREDICTED: hypothetical protein [Vitis vinifera]	236	1e-60	
AVR3aPI-12	ref XP_002270696.1 PREDICTED: hypothetical protein [Vitis vinifera]	508	4e-142	Protein of unknown function DUF828, plant (InterPro:IPR008546)
AVR3aPI-13	ref XP_002275990.1 PREDICTED: hypothetical protein isoform 2 [Vitis vinifera]	344	3e-93	Cysteine synthase/cystathionine beta-synthase P-phosphate-binding site (InterPro:IPR001216)

Supplementary Figure Legends

Fig. S1 Alignment of CMPG1 protein sequences used in this study, including Δ N-StCMPG1a from *Solanum tuberosum*, identified in the original Y2H screen, a second CMPG1 sequence from *Solanum tuberosum* (StCMPG1b), two from *Nicotiana benthamiana* (Nb) and one from *Solanum lycopersicon* (Sl).

Fig. S2 AVR3a strongly interacts with and stabilizes CMPG1 *in planta*.

(A) Western blots probed with anti-myc and anti-FLAG antibodies following transient co-expression at 5 days post-agroinfiltration (dpi) of FLAG-AVR3a^{KI}, FLAG-AVR3a^{EM} or FLAG-AVR3a^{KI/Y147del} with two full length (55 kDa) CMPG1 proteins from *Nicotiana benthamiana* (4x-myc-NbCMPG1a, 4x-myc-NbCMPG1b) or one from tomato (4x-myc-SlCMPG1a) (Fig. S1). Sizes are indicated in kDa. Protein loading is shown by coomassie blue stain (CBB). (B) Expression of *R3a* alone, and co-expression of CFP-Avr3a^{KI} (KI), CFP-Avr3a^{EM} (EM) and CFP-Avr3a^{KI/Y147del} (Δ 147) with *R3a* in *N. benthamiana*. As expected, both CFP-AVR3a^{KI} and CFP-AVR3a^{KI/Y147del} triggered R3a-mediated cell death, whereas CFP::AVR3a^{EM} did not, demonstrating that this activity was retained by the N-terminal CFP fusions. (C) Western blot probed with anti-GFP antibody following expression in *N. benthamiana* of CFP-Avr3a^{KI} (1), CFP-Avr3a^{EM} (2), CFP-Avr3a^{KI/Y147del} (3). Protein from uninfiltrated leaf is shown in (4). Protein loading is indicated by Ponceau staining (PS). All three constructs generated intact CFP fusions *in planta*. (D) Co-expression of CFP-AVR3a^{KI} (KI), CFP-AVR3a^{EM} (EM) and CFP-AVR3a^{KI/Y147del} (Δ 147) with full length StCMPG1b-YFP visualized at 3 dpi using confocal microscopy. Upper panels show CFP fluorescence, lower panels show YFP. Whereas CFP fluorescence was similar in each experiment, indicating similar levels of CFP-AVR3a^{KI}, CFP-AVR3a^{EM} and CFP-AVR3a^{KI/Y147del} proteins, CMPG1-YFP fluorescence was significantly stronger following co-expression with CFP-AVR3a^{KI} than with CFP::AVR3a^{EM}, and barely detectable with CFP-AVR3a^{KI/Y147del}, further indicating that AVR3a^{KI} more strongly stabilizes CMPG1. (E) Bimolecular fluorescence complementation, following co-expression of CMPG1-YN with YC-AVR3a^{KI}, YC-Avr3a^{KI/Y147del} or free YC, with or without expression also of untagged AVR3a^{KI} (as indicated). Although the expression of AVR3a^{KI} will stabilize CMPG1-YN, split YFP fluorescence is stronger with YC-AVR3a^{KI} than with YC-Avr3a^{KI/Y147del}. The latter shows similar fluorescence to that observed between CMPG1-YN and free YC, which can therefore be regarded as background YFP reconstitution. Scale bars are 200 μ m.

Fig. S3 CMPG1 is not required for recognition by R3a

(A) Infiltration of a range of INF1 protein dilutions into wild-type tobacco and a tobacco CMPG1-RNAi line previously used (1). (B) Co-expression, by *Agrobacterium* delivery, of Avr3a^{KI}, Avr3a^{EM}, Avr3a^{KI/Y147del} or pGR106 vector control with *R3a* in wild-type tobacco and a CMPG1-RNAi line. Whereas AVR3a^{KI/Y147del} fails to suppress INF1-triggered cell death or to interact with CMPG1 (Fig. 1, main text), it nevertheless still triggers R3a-mediated cell death (2; Fig. S2), suggesting that the R3a HR is independent of CMPG1. Whilst infiltration with a range of INF1 concentrations yielded cell death, as expected, only in WT tobacco (Fig. S3A), co-expression of either Avr3a^{KI} or Avr3a^{KI/Y147del} forms with *R3a* yielded an HR in both WT and CMPG1-RNAi tobacco plants, (Fig. S3B). These results indicate that R3a-mediated cell death is independent of CMPG1.

1. Gonzàles-Lamothe, R., Tsitsigiannis, D.I., Ludwig, A.A., Panicot, M., Shirasu, K., and Jones, J.D.G. (2006). The U-box protein CMPG1 is required for efficient activation of defence mechanisms triggered by multiple resistance genes in tobacco and tomato. *The Plant Cell*, *18*, 1067-1083.
2. Bos, J.I.B., Chaparro-Garcia, A., Quesada-Ocampo, L.M., McSpadden Gardener, B.B., and Kamoun, S. (2009). Distinct amino acids of the *Phytophthora infestans* effector AVR3a condition activation of R3a hypersensitivity and suppression of cell death. *Mol. Plant-Microbe Interact.*, *22*, 269-281.

Fig. S4 The roles of CMPG1 during *P. infestans* infection. (A) *NbCMPG1a* is induced >90-fold only 60 minutes after inoculation of a mixture of *P. infestans* sporangia and zoospores onto leaves of *N. benthamiana*. (B) Real-time RT-PCR analysis of *NbCMPG1* expression across a time course from 1 to 5 days post-inoculation (dpi), relative to day 0 (sampled 5 minutes after inoculation of *Phytophthora infestans* sporangia/zoospores), which was given a value of 1. *NbCMPG1* transcripts accumulated to a level 9-fold higher at 3 dpi than at time 0, before decreasing at 4 to 5 dpi, indicating a tightly-regulated peak of induction at 3 dpi. (C) Real-time RT-PCR analysis of *Avr3a* expression from 1 to 5 dpi, relative to its expression in sporangia (S), which was given a value of 1, and was relative to the constitutively expressed *ActA* gene (3). As observed previously, *Avr3a* was up-regulated early, at 1 dpi and, although transcript accumulation was considerably higher than observed in sporangia, expression nevertheless declined steadily throughout the 5 days of infection. (D) Real-time RT-PCR analysis of *INF1* expression from 1 to 5 dpi, measured as in (C). *INF1* expression at 1 dpi was approximately half that observed in *in vitro* sporangia but, by 2 dpi, had decreased considerably, as previously reported (4). From 2 dpi, in the biotrophic phase, there was then a dramatic increase in *INF1* expression at 3 and 4 dpi. *INF1* mRNA accumulation then decreased by 5 dpi. (E) Real-time RT-PCR analysis of *cdc14* expression from 1 to 5 dpi, measure as in (C). The *P. infestans* gene *Cdc14*, the expression of which is restricted to the onset of sporangial development (5) was significantly up-regulated at 5 dpi, indicating that sporulation occurs after *CMPG1* up-regulation.

3. Avrova, A.O., Venter, E., Birch, P.R.J., and Whisson, S.C. (2003). Identification and quantification of *Phytophthora infestans* genes expressed prior to or during potato infection. *Fungal Genetics and Biology*, *40*, 4-14.
4. Kamoun, S., Van West, P., de Jong, A.J., de Groot, K.O., Vleeshouwers, V.G.A.A., and Govers, F. (1997). A gene encoding a protein elicitor of *Phytophthora infestans* is down-regulated during infection of potato. *Mol. Plant-Microbe Interact.*, *10*, 13-20.
5. Ah Fong, A.M., and Judelson H.S. (2003). Cell cycle regulator *cdc14* is expressed during sporulation but not hyphal growth in the fungus-like oomycete *Phytophthora infestans*. *Mol. Microbiol.* *50*, 487-494.

Fig. S5 Virus induced gene silencing of *NbCMPG1* leads to reduced *P. infestans* sporulation and lesion development. (A) Diagram of *CMPG1* showing the relative locations of the U-box-encoding region, the hairpin sequence for RNAi in tobacco (1), the region of *NbCMPG1a* used for VIGS (*CMPG1*) and the locations of primers used for real time RT-PCR (arrows). Numbers represent nucleotide positions. (B) Images of *N. benthamiana* leaves expressing TRV::*GFP*, 6 dpi after inoculation of *P. infestans* 88069 sporangia (left panels) and these leaves stained with trypan blue (right panels). (C) Images of *N. benthamiana* leaves expressing TRV::*NbCMPG1*, 6 dpi after inoculation of *P. infestans* 88069 sporangia

(left panels) and these leaves stained with trypan blue (right panels). Whilst staining indicates substantial infection in all leaves, sporangia development is considerably more in TRV::*GFP* leaves.

Fig. S6 Transient expression of *CFP-AVR3a^{KI}* is silenced 5 days after agroinfiltration. A time-course of *CFP-AVR3a^{KI}* fluorescence without (upper panels) or with (lower panels) the silencing suppressor P19. Without P19, *CFP-AVR3a* fluorescence is barely detectable at 5-6 days post-infiltration (dpi), indicating that expression of this construct is silenced, as fluorescence in the presence of P19 remains clearly detectable. The size marker indicates 200 μ m.

Fig. S7 *AVR3a^{KI}* and *AVR3a^{EM}* complement loss of virulence in *P. infestans* silenced line CS12, but *AVR3a^{KI}Y147deletion* mutant does not. Virulence of the *P. infestans* silenced line CS12 was restored following transient agroexpression of *AVR3a^{EM}* (EM) (upper panel) or *AVR3a^{KI}* (KI) (lower panel) in one half of leaves. No such complementation was observed following agroexpression of *AVR3a^{KIY147del}* mutant (Δ Y147) in adjacent halves of these leaves. *P. infestans* sporangia and zoospores were spot-inoculated 2 days after agroinfiltration of the constructs and the leaves were stained with trypan blue five days later (right panels). This experiment was repeated four times with 2-3 leaves on 6-8 plants for each construct and gave reproducible results.

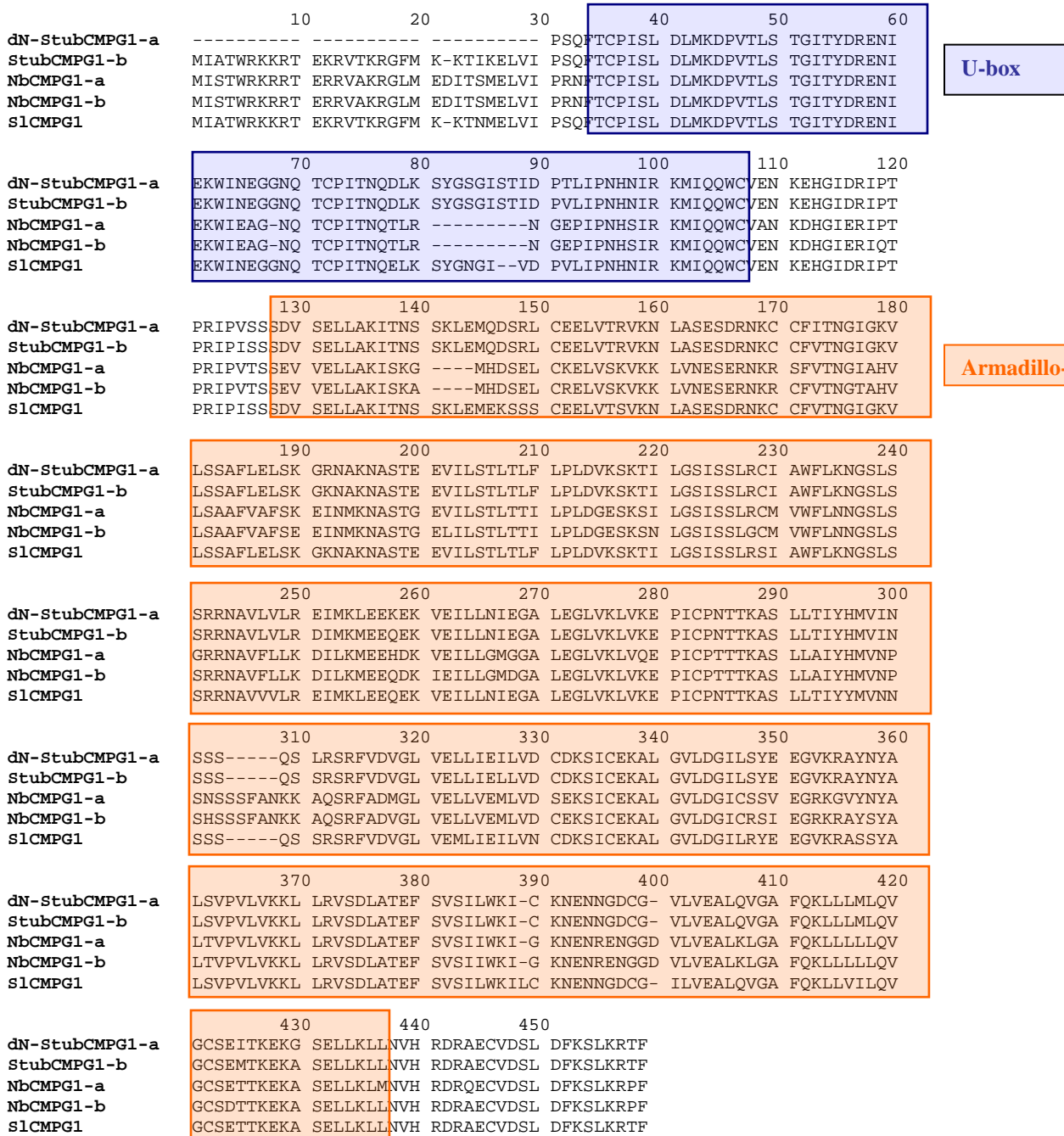


Fig. S1

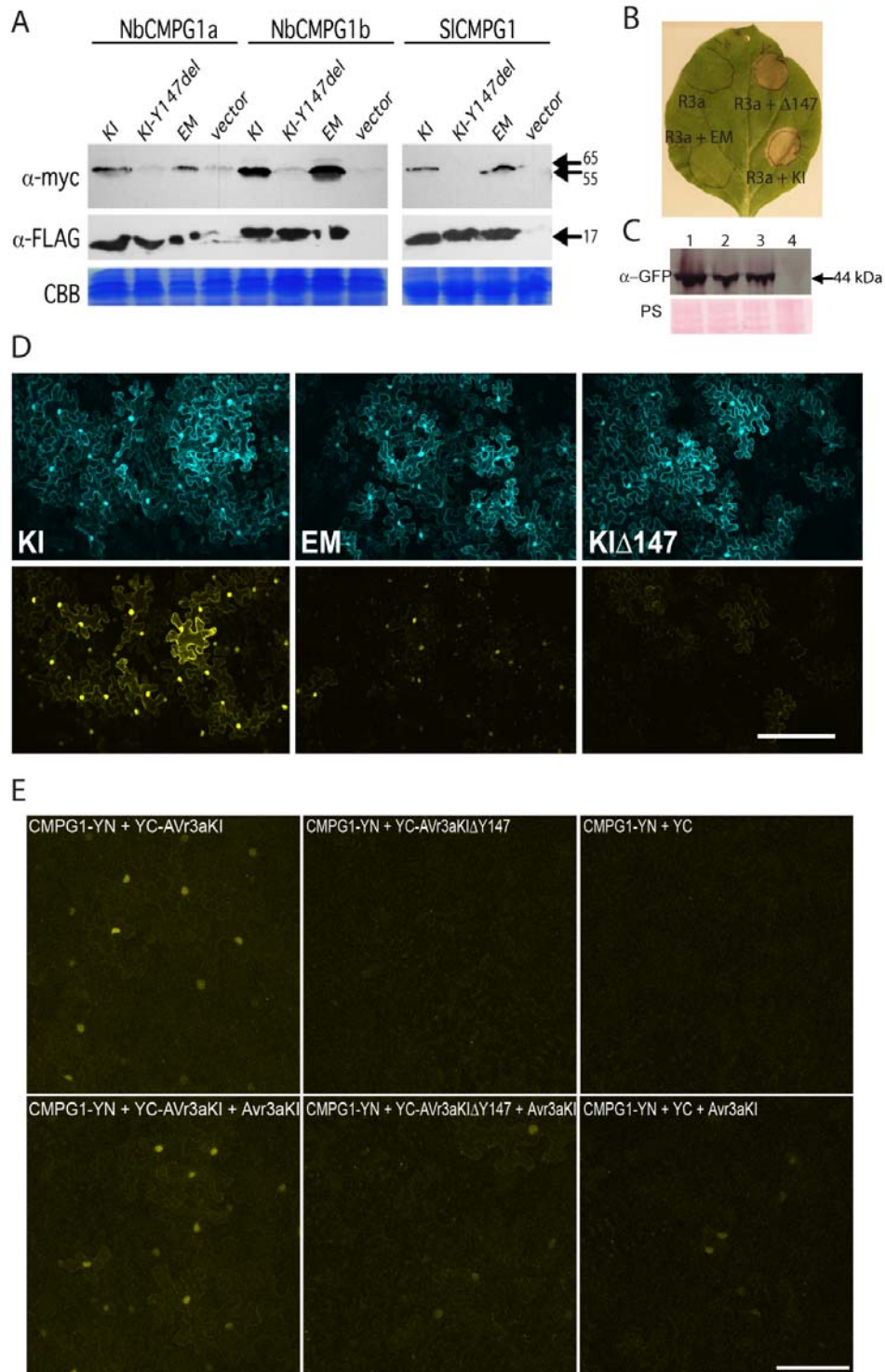


Fig. S2

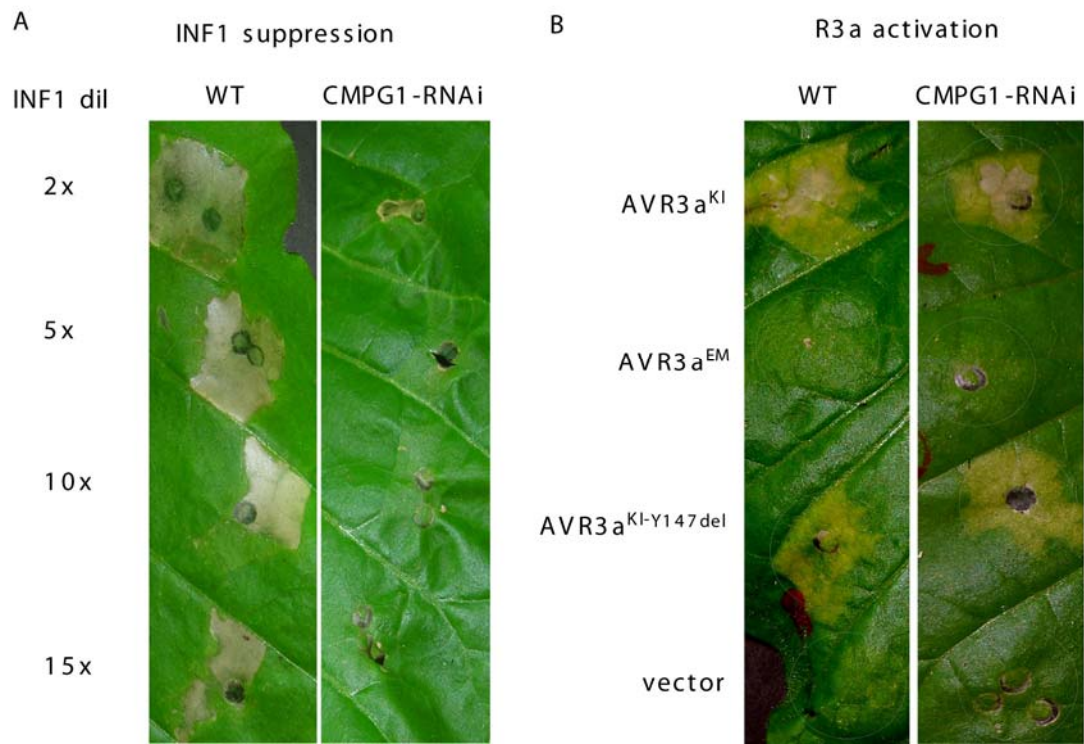


Fig. S3

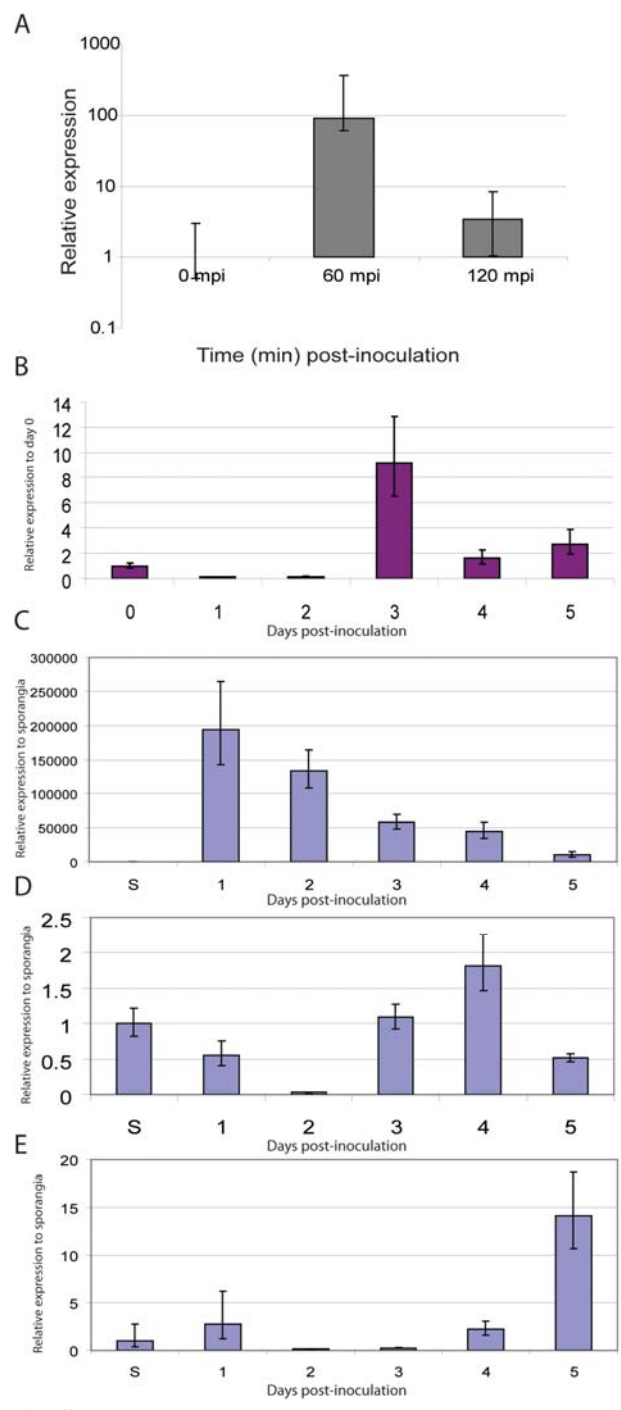
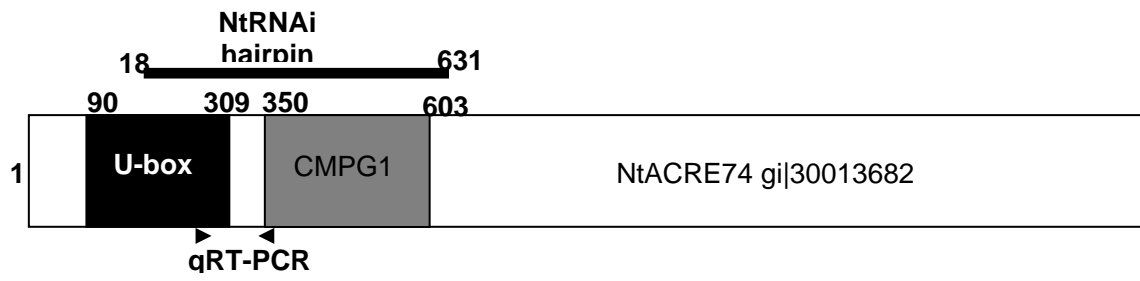
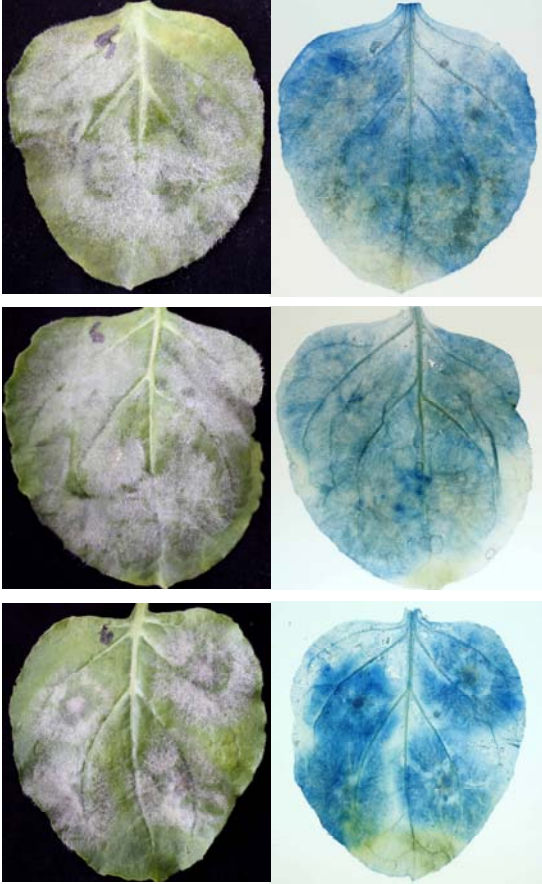


Fig S4

A.



B



C

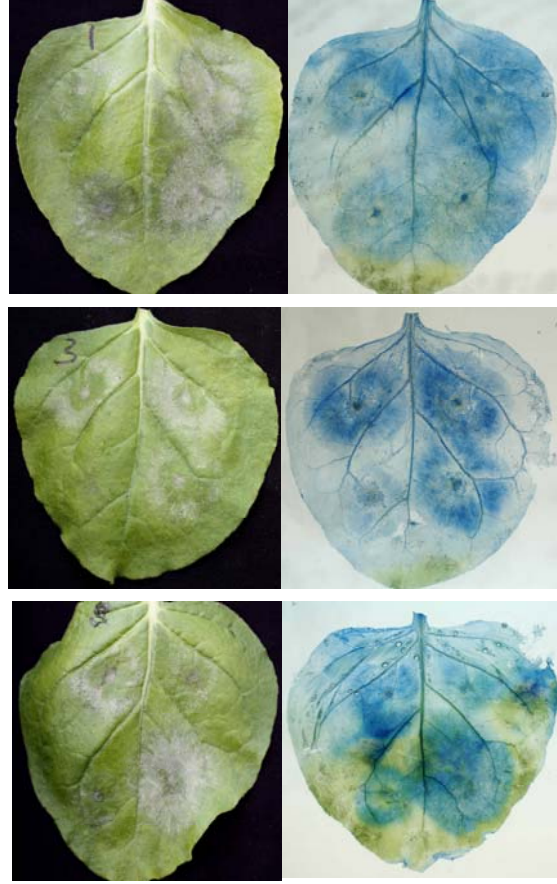


Fig. S5

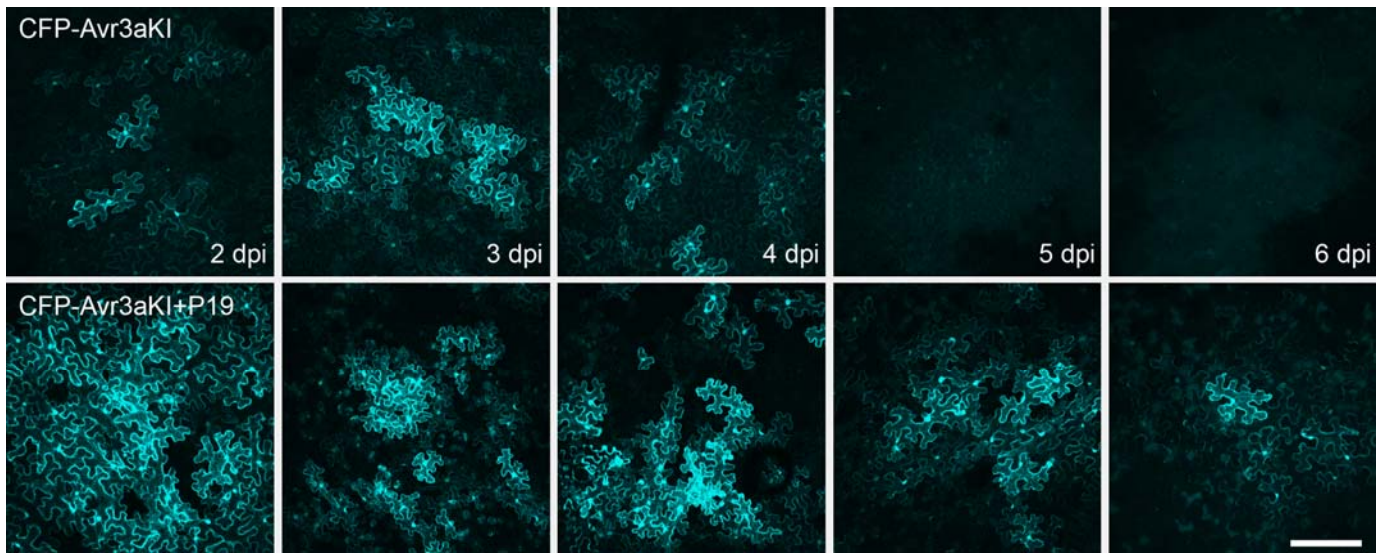


Fig. S6

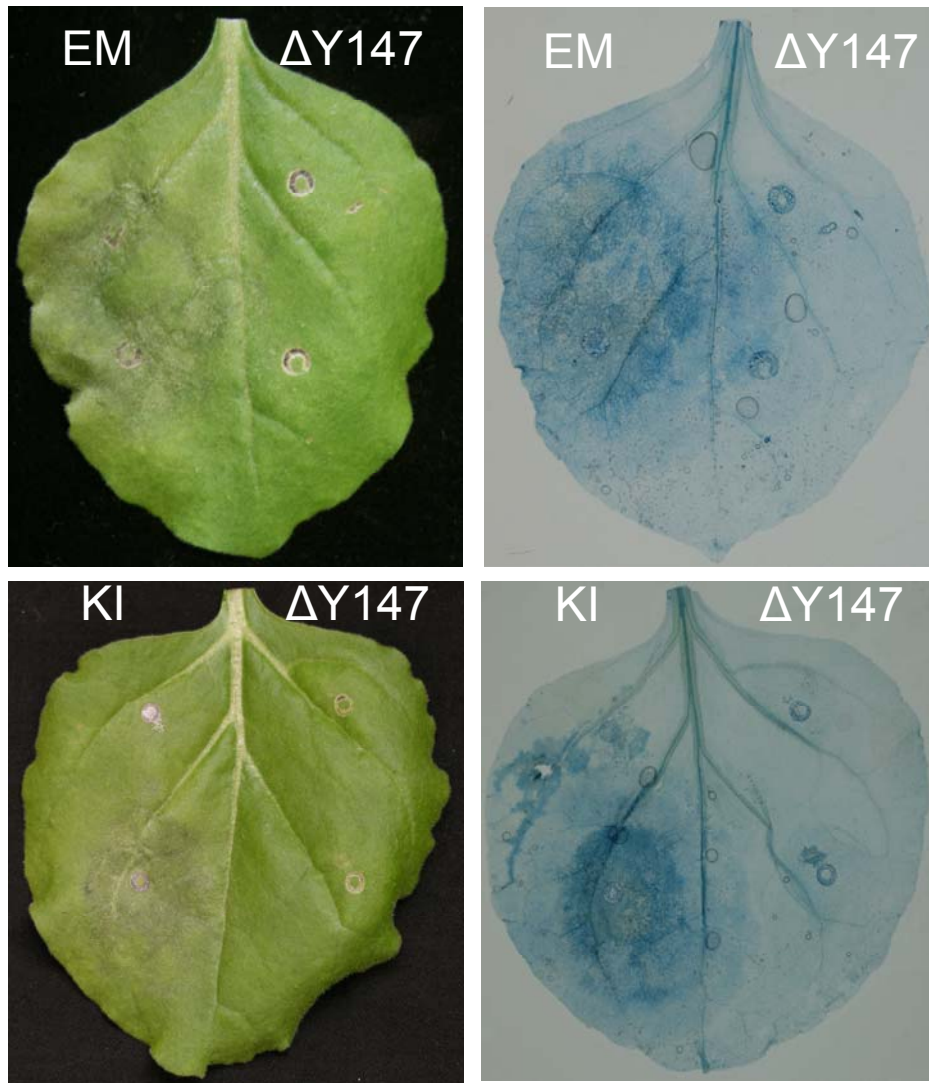


Fig. S7